1 Full Title: Meiotic DSB repair DNA synthesis tracts in *Arabidopsis thaliana*

2 Short Title: SPO11-dependent meiotic DNA synthesis.

3

4 **Authors:** Miguel Hernández Sánchez-Rebato[1&], Veit Schubert[2], Charles I. White[1]*

5

6 Affiliations:

7 [1] Institut de Génétique, Reproduction et Développement, CNRS UMR 6293, INSERM U1103,

8 Université Clermont Auvergne, 28, place Henri Dunant,

9 63001 Clermont-Ferrand, France.

10 [2] Leibniz Institute of Plant Genetics and Crop Plant Research (IPK) Gatersleben, D-06466 Seeland,

11 Germany

12 [&]Current address: Centro de Biología Molecular Severo Ochoa,

13 Calle Nicolás Cabrera 1, 28049 Madrid, Spain

14

15 * Corresponding author.

16 E-mail: charles.white@cnrs.fr

17

18 **Keywords:** Meiosis, Recombination, DNA synthesis, DSB repair, SPO11

19

Abstract

We report here the successful labelling of meiotic prophase I DNA synthesis in the flowering plant, *Arabidopsis thaliana*. Incorporation of the thymidine analogue, EdU, enables visualisation of the footprints of recombinational repair of programmed meiotic DNA double-strand breaks (DSB), with ~400 discrete, SPO11-dependent, EdU-labelled chromosomal foci clearly visible at pachytene and later stages of meiosis. This number equates well with previous estimations of 200-300 DNA double-strand breaks per meiosis in Arabidopsis, confirming the power of this approach to detect the repair of most or all SPO11-dependent meiotic DSB repair recombination. The chromosomal distribution of these DNA-synthesis foci accords with that of early recombination markers and MLH1, which marks Class I crossover sites, colocalises with the EdU foci.

It is currently estimated that ~10 cross-overs (CO) and an equivalent number of non-cross-overs (NCO) occur in each Arabidopsis male meiosis. Thus, at least 90% of meiotic recombination events, and very probably more, have not previously been accessible for analysis. Visual examination of the patterns of the foci on the synapsed pachytene chromosomes corresponds well with expectations from the different mechanisms of meiotic recombination and notably, no evidence for long Break-Induced Replication DNA synthesis tracts was found. Labelling of meiotic prophase I, SPO11-dependent DNA synthesis holds great promise for further understanding of the molecular mechanisms of meiotic recombination, at the heart of reproduction and evolution of eukaryotes.

Author Summary

Sexual reproduction involves the fusion of two cells, one from each parent. To maintain a stable chromosome complement across generations, these specialized reproductive cells must be produced through a specialized cell division called meiosis. Meiosis halves the chromosome complement of gametes and recombines the parental genetic contributions in each gamete, generating the genetic variation that drives evolution. The complex mechanisms of meiotic recombination have been intensely studied for many years and we now know that it involves the repair of programmed chromosomal breaks through recombination with intact template DNA sequences on another chromatid. At the molecular level, this is known to involve new DNA synthesis at the sites of repair/recombination and we report here the successful identification and characterisation of this DNA neo-synthesis during meiosis in the flowering plant, Arabidopsis. Both the characteristics and numbers of these DNA synthesis tracts accord with expectations from theory and earlier studies. Potentially applicable to studies in many organisms, this approach provides indelible footprints in the chromosomes and has the great advantage of freeing researchers from dependence on indirect methods involving detection of proteins involved in these dynamic processes.

60 ## Introduction

61 Meiosis is the specialised cell division that halves chromosome numbers during the
62 production of gametes, essential for the maintenance of stable ploidy across generations in
63 sexually-reproducing organisms. In contrast to mitosis, in which duplication of the genome is
64 followed by a single cellular division, meiosis involves one round of DNA replication followed by
65 two rounds of division. Separating sister chromatids to opposite poles, the second meiotic
66 division is, in broad terms, analogous to mitosis. Balanced chromosomal segregation during the
67 first division however requires that homologous chromosomes recognise each other, pair and
68 orient themselves on the spindle so that the two members of each pair move to opposite poles
69 during anaphase. This is ensured by the programmed induction of homologous recombination
70 through the induction and repair of DNA double-strand breaks (DSB) during the first meiotic
71 prophase.

72 This programmed, highly regulated process of DNA damage and repair is essential for
73 proper meiotic chromosome alignment and segregation and thus fertility in eukaryotes, with
74 some known exceptions, notably *Drosophila* and *C. elegans* (see review by [1]). Following the
75 programmed induction of DSB by the SPO11 complex, the cleaved DNA ends are resected to
76 produce 3'-ssDNA overhangs, onto which the recombinases DMC1 and RAD51 are loaded to
77 form presynaptic nucleoprotein filaments. These presynaptic nucleofilaments are the active
78 molecular species in the search for, and invasion of an intact homologous DNA template, the first
79 steps of DNA repair via homologous recombination. DNA synthesis then extends the invading 3'
80 end across the template and the joint-molecule intermediate structures are further processed to

81 yield the two main products of HR-mediated DSB repair: gene conversions associated with
82 reciprocal exchange of their flanking sequences (crossovers, CO), or not (non-crossovers, NCO).

83 DNA synthesis is thus inherent to DSB repair via homologous recombination. In the 1960s,
84 studies based on incorporation of H3-thymidine and C14-thymidine into newly synthesised DNA
85 gave evidence for meiotic prophase I DNA synthesis in the plants *Lilium longiflorum* and *Trillium*
86 *erectum*, the amphibian *Triturum viridescens*, mice and humans [2–6]. These early studies have
87 since been extended to show association of DNA synthesis with pachytene recombination
88 nodules in *Drosophila* female meiosis and with the synaptonemal complex in mouse
89 spermatocytes [7,8].

90 Labelling with 5-bromo-2′-deoxyuridine (BrdU) in budding yeast has been used to confirm
91 the presence of SPO11-dependent meiotic prophase DNA synthesis [9]. The authors
92 characterized both single-molecule BrdU tracts at a recombination hotspot and the timing of
93 their appearance in relation to other meiotic features. Observation of SPO11-dependent, BrdU
94 labelling pattern has also been described in *Tetrahymena* [10] but, to our knowledge, no further
95 data has been published in other organisms. In Arabidopsis, incorporation of BrdU or 5-ethynyl-
96 2'- deoxyuridine (EdU) during pre-meiotic S-phase has been used to establish the meiotic
97 timeline of meiosis in Arabidopsis pollen mother cells (PMC) [11–13]. There are thus far no
98 reports of labelling non-S-Phase DNA synthesis during Arabidopsis meiosis.

99 The induction of synchronous meiosis in populations of cells has been key to a number of
100 major advances in understanding of the molecular processes that make up the meiotic division
101 [14–18]. However, such direct approaches have not been available in other organisms and this
102 has resulted in significant gaps in understanding. A clear example of this is seen in the flowering

103 plant, *A. thaliana*. Estimations of numbers of SPO11-induced DSB in Arabidopsis pollen mother
104 cells (PMC, male meiosis) are ~200-300 per meiosis. Of these, ~10 yield inter-homologue CO and
105 another 10 have been shown to give inter-homologue NCO [19,20]. Thus, the repair outcome of
106 at least 90% of meiotic DSB in Arabidopsis is not known. The situation is strikingly different in
107 budding yeast with 66 NCO plus 90.5 CO estimated per meiosis, the sum of which is very close to
108 the estimated 140-170 meiotic DSB. Similarly in mouse, 273 NCO plus 27 CO sum close to the
109 estimated 200-400 meiotic DSB [21–24].

110 Detection of recombination-associated DNA synthesis tracts offers an attractive path to
111 understand the mechanisms underlying these "invisible" meiotic recombination events in
112 Arabidopsis and potentially in other organisms. We present here the successful labelling of
113 SPO11-dependent, meiotic prophase I DNA synthesis by EdU incorporation in Arabidopsis PMC.

114

115

116 Results

117 EdU labelling of DSB repair-associated DNA synthesis

118 In Arabidopsis, while each inflorescence contains flower buds bearing PMC at different pre-
119 meiotic and meiotic stages, the PMC of the anthers of a given flower bud are nearly synchronous
120 [25,26]. Along with the sequence of cytologically distinguishable meiotic stages in the buds of a
121 given inflorescence, in practice it is relatively straightforward to classify PMC subpopulations
122 within the meiotic timeline.

123 Timelines of Arabidopsis male meiosis concord that pre-meiotic G2 phase lasts 7-10 hours
124 and that pollen mother cells advance from the beginning of leptotene to the end of pachytene in
125 19 to 21 hours [11–13,27](summarized in Figure 1). Subsequent stages of meiosis are
126 considerably faster, with post-pachytene meiosis estimated to take from 2.7 to 9 hours. Given
127 that meiotic DSB formation begins at the onset of prophase I (early leptotene) and continues for
128 a few hours [28], any meiotic prophase I DSB-repair DNA synthesis should occur at least 7-10
129 hours after the end of pre-meiotic S-phase. We thus decided to incubate the inflorescences with
130 the nucleoside analogue for a 24-hour pulse to entirely cover the prophase I DSB repair-
131 associated DNA synthesis window. Given the relative synchrony of progression through meiosis
132 of the PMC from a given flower bud, the easily identifiable appearance of S-phase labelling and
133 the possibility to easily situate subpopulations of meiotic cells in the temporal meiotic sequence,
134 it seemed reasonable to expect that we would be able to exclude S-phase labelled meioses, and
135 thus focus our analyses on those labelled during Prophase I.

136 Notwithstanding the current absence of direct evidence of the timing of occurrence of
137 meiotic recombination intermediates in Arabidopsis, DAPI staining and immunolocalisation of
138 meiotic proteins implicated in early invasion intermediates (RAD51/DMC1), joint molecules
139 (MSH4, early HEI10) and resolution (MLH1, late HEI10) give a clear picture of the progression of
140 key events through meiotic prophase I. In pachytene, when synapsis is complete, mean numbers
141 of MLH1 foci correspond to the number of Class I crossovers (~90% of total CO), measured by
142 counting of chiasmata at metaphase I. In analogy to organisms for which recombination
143 intermediates can be tracked directly, it is reasonable to assume that most recombination events
144 are either resolved or close to resolution at pachytene in Arabidopsis.

145 As summarised in Figure 1 , inflorescences were thus incubated with EdU for 24 hours to
146 ensure coverage of the window of DSB repair-associated DNA synthesis through prophase I up to
147 the end of pachytene. Pachytene cells observed at the end of the 24-hour pulse would have
148 traversed prophase I up to that point in the presence of the analogue. As mentioned above,
149 nuclei with pre-meiotic S-phase labelling were easily identified and excluded from the analysis.

150

151 **Non-replicative DNA synthesis tracts are present from pachytene until the end of meiosis**

152 Early prophase I meiocytes, including cells in leptotene and zygotene, showed complete or
153 extensive EdU labelling of their chromosomes (Figure 2a). This replicative labelling confirms, as
154 expected, that they had passed through pre-meiotic S-Phase during the EdU pulse [11–13,29,30].
155 Furthermore, nuclei with partial replicative labelling of DAPI-dense, late replicating
156 heterochromatic regions were observed, as expected for cells that were in mid/late S-phase at
157 the beginning of the EdU pulse (second row of Figure 2a) [30–33].

158 In striking contrast, pachytene nuclei showed faint, discrete foci of a considerably smaller
159 size (Figure 2a Pachytene, see also Figure 4a and Figure S1). These foci are very faint through the
160 microscope eyepiece, but are clearly visible when the images are processed. This difference in
161 labelling intensity between S-phase and prophase EdU incorporation is not unexpected,
162 considering that the latter would correspond to DNA synthesis tracts of tens to a few thousands
163 of base pairs, while replicative DNA synthesis would range from megabase-long late-replicating
164 regions to the whole genome (4C ≈ 520 Mb in these prophase I nuclei) [34]. We note also the
165 presence of labelled mitochondria in these images, confirming their replication during pre-

166 meiotic G2 and/or meiotic prophase I cells. These labelled mitochondria, clearly visible from
167 pachytene on, are also present at earlier stages, but are not readily visible due to the very strong
168 fluorescence of the S-phase replicative nuclear labelling (Figure 2).

169 The EdU foci observed in pachytene cells appear well-distributed across the chromosomes,
170 but are less present in DAPI-dense, heterochromatic regions (Figure 2a Pachytene, Figure 4a).
171 Furthermore, given the tighter-packed DNA in these regions, the observed lesser density of EdU
172 foci is presumably an underestimation. This pattern of foci concords with genetic crossover
173 mapping, studies of meiotic DSB (SPO11-oligo sequencing) and immunofluorescence studies of
174 the distributions of early recombination proteins, all of which show meiotic recombination to
175 follow a relatively even distribution across the Arabidopsis genome, with the exception of
176 (heterochromatic) centromeric regions which have significantly lower densities of SPO11-oligos
177 and crossovers [34–36].

178 As summarised in Figure 1, based on published timelines [11–13,27] and our own
179 measurements, a meiocyte observed at the telophase II/tetrad stage would have been at
180 leptotene/zygotene at the beginning of the 24-hour EdU pulse. We had thus good reason to
181 expect that prophase I EdU foci would be observable in all meiotic stages up to the end of
182 meiosis. This was indeed the case, with EdU foci visible from pachytene to the end of meiosis
183 (telophase II/tetrad Figure 2). Meiotic chromosomes condense progressively as they traverse
184 prophase I, evolving from a mass of hardly-distinguishable thin fibres at early leptotene to thick
185 synapsed fibres in pachytene and to individualised dense bivalents with a more polygonal shape
186 at metaphase I. This condensation produces significant shortening of the chromosomes and
187 results in changes of the visual character of the EdU signals. While most EdU foci at pachytene

188 appear as discrete spots, they merge into larger patches at diplotene and this continues through
189 diakinesis, up to the greatest condensation at metaphase I (Figure 2, diplotene-metaphase I).
190 Furthermore, heterochromatic, centromeric regions become more easily identifiable when
191 bivalents individualize at diakinesis and the relatively low density of EdU signals in these regions
192 becomes clearly visible. This is even more pronounced at metaphase I, with clear visual
193 differentiation between the centromeric and pericentromeric regions of the two homologous
194 chromosomes of each bivalent. Finally, the EdU signals are observed throughout the second
195 meiotic division, changing their appearance with evolving chromosome condensation and shape
196 in a way similar to that seen during the first meiotic division (Figure 2, prophase II-tetrad).
197

198 Prophase I DNA synthesis is SPO11-dependent

199 Meiotic recombination is initiated by the induction of DNA DSB by the SPO11 complex at the
200 beginning of meiotic prophase I. To verify that the discrete non-replicative DNA synthesis tracts
201 observed at pachytene and subsequent stages originate from SPO11-dependent meiotic DSB
202 repair, we carried out this analysis in parallel in *spo11-1* mutant plants [37] (Figure 3).
203 Pachytene images were analysed with the IMARIS software package (Bitplane AG, Oxford
204 Instruments, UK) *Spots* function. EdU foci were selected based on diameter and mean intensity
205 in the EdU channel, and filtered to retain only those colocalising with chromosome fibres (mean
206 intensity cutoff in the DAPI channel). A high-cut filter of mean intensity in the EdU channel was
207 also applied to filter out the much-brighter organellar foci.

208 WT pachytenes show 409.5 ± 7.96 EdU foci per nucleus (mean ± SEM; n = 45 nuclei; Figure
209 2, Figure S1), with counts ranging from 323 to 510 (plus one outlier with 263). Ten of the 45
210 image stacks analysed were acquired via 3D-SIM, for comparison with the Zeiss LSM
211 800/Airyscan confocal image stacks and to confirm that we were not missing foci. WT cells
212 imaged with 3D-SIM had a mean 400.6 ± 14.74 EdU foci (n = 10) while those imaged with the
213 confocal microscope had a mean of 412.1 ± 9.38 EdU foci (n = 35). Hence, no significant
214 difference was observed between both imaging systems (unpaired t-test; p = 0.55) (Figure 4).

215 In *spo11-1* plants, 39.2 ± 2.83 EdU foci per cell (mean ± SEM; n = 35 cells; Figures 3, 4) were
216 detected in zygotene/pachytene nuclei. Thus, some EdU foci were detected in *spo11-1* meioses,
217 but in significantly lower numbers and, in general, considerably smaller and weaker than the foci
218 in the WT. A similar signature could be observed in *spo11-1* cells at subsequent meiotic stages
219 (Figure 3, diakinesis to Telophase II), with some EdU foci detected but in much lower numbers.
220 This ~10-fold reduction in mean numbers of foci with respect to the WT is highly significant
221 (unpaired t-test; $p < 0.0001$) and confirms the SPO11-dependence of the great majority of the
222 observed pachytene EdU foci. That the expected S-phase EdU labelling was observed in early
223 prophase I *spo11-1* PMC nuclei (Figure 3, early PI, mid PI, second row) and organellar EdU
224 labelling was comparable in *spo11-1* and WT meioses (Figures 2, 3), confirms that the EdU
225 labelling pulse worked as expected in both WT and *spo11-1* plants.

226 In interpreting these numbers it is important to note that although Arabidopsis *spo11*
227 meiosis does complete and produce (mostly inviable) pollen, chromosome pairing and synapsis
228 are very severely reduced in *spo11* meiosis and the zygotene/pachytene stages are only
229 identifiable by their characteristic chromosome condensation and their temporal positioning

230 [37]. Thus, *spo11-1* PMC at leptotene can be differentiated from the zygotene-like state by the
231 condensation of the chromosomes (thickness of the fibres) and the clustering of DAPI-dense
232 regions. Also, *spo11-1* zygotene/pachytene-like cells that do not show S-phase EdU labelling are
233 in a more advanced state that those that do show it, as they would have completed S-phase at
234 the beginning of the pulse (Figure 3a, mid PI, third row vs second row). Identification of later
235 meiotic stages in *spo11-1* meioses presents no difficulties (Figure 3).

236

237 **Prophase I DNA synthesis patterns mirror meiotic recombination features**

238 Meiotic recombination models predict different patterns of DNA synthesis tracts depending
239 on how recombination intermediates are formed and resolved. Non-crossover events generated
240 by either synthesis-dependent strand annealing (SDSA) or dHJ dissolution recombination, both
241 expected to produce DNA synthesis tracts in only one of the two implicated chromatids and thus
242 in only one of the homologous chromosomes in interhomologue recombination. On the other
243 hand, dHJ resolution resulting in either crossover or non-crossover products would generate
244 DNA synthesis tracts in both participating chromatids - and both chromosomes in
245 interhomologue events.

246 The expected patterns of resulting EdU foci are shown schematically in Figure 5a and
247 examples of segments of the synaptonemal complex (SC) from SIM pachytene micrographs are
248 shown in Figure 5b. The paired, homologous chromosomes are clearly distinguishable in these
249 images, permitting a first analysis of different patterns of EdU foci. No obvious bias is visible in
250 the disposition of Individual EdU foci in these images. Foci are seen at both the internal (facing

251 the homologous chromosome) and external faces of the paired chromosomes in the SC fibre, as
252 well as in the middle of the SC (Figure 5).

253 Differences can however be seen when EdU foci are analysed with respect to adjacent foci,
254 with three clear configurations of pairs of foci, examples of which are circled on the images
255 shown in Figure 5b:

256 Class (1) isolated individual foci located on one of the two homologues (one SC lateral
257 axis; Fig. 5b, white circle).

258 Class (2) "pairs" of foci on one of the two homologues (one SC lateral axis; Fig. 5b, green
259 circle).

260 Class (3) "pairs" of foci on the two homologues (both SC lateral axes; Fig. 5b, yellow
261 circle).

262 Further examples of these patterns can be found in the pachytene images of Figure S2.

263 Finally, we note the absence of the long labelling tracts expected from BIR recombination,
264 implying that such events are either rare or "short", or both, in Arabidopsis meiosis.

265

266 **Prophase I DNA synthesis colocalize with class I crossovers**

267 As the SPO11-dependent, meiotic prophase I DNA synthesis foci result from recombinational
268 repair of meiotic DSB, genetic crossovers should co-localize with a subset of these EdU foci. Class
269 I CO are detectable cytologically in Arabidopsis by the immunolocalization of proteins such as
270 MLH1.

271 Combining labelling of EdU tracts with immunolocalization of MLH1 (Figure 6) gave 7.86 ±
272 0.24 (mean ± SEM; n = 29) MLH1 foci per WT pachytene, as expected [38]. 95.6% (n=228) of all
273 MLH1 foci colocalized with an EdU focus and the remaining 4.4% were adjacent to one. Although
274 this conclusion must be tempered due to the high number of EdU foci in these images, Arabidopsis
275 Class I CO are thus physically associated with the prophase I DNA synthesis tracts at this level of
276 resolution.

277

278 ## Discussion

279 ### Identification of meiotic DNA repair-associated DNA synthesis tracts

280 We present here the labelling and characterisation of SPO11-dependent, meiotic prophase I
281 DNA synthesis tracts through incorporation of the thymidine analogue EdU in pollen mother cells
282 of Arabidopsis plants. By labelling DNA synthesis associated with the repair of meiotic DSB, this
283 approach holds great promise for the future understanding of recombination patterns and
284 mechanisms, notably for studies of NCO and sister-chromatid exchange (SCE) recombination. For
285 practical reasons, molecular and genetic studies of meiotic recombination have essentially been
286 focussed on events implicating the transfer of DNA sequence polymorphisms between the two
287 recombining DNA molecules. The necessary presence of such polymorphism has, for instance,
288 complicated significantly the analysis of the roles of meiotic SCE [39–46] and while EdU labelling
289 has recently been applied to analysis of meiotic sister-chromatid CO in *C. elegans* (Almanzar *et*
290 *al*, 2021; Toraason *et al*, 2021; Billmyre & Hughes, 2021), this approach does not appear adapted
291 to the study of NCO.

292 Detection of NCO events in Arabidopsis has been elusive. Mapping NCO genome-wide by
293 sequencing Arabidopsis tetrads has estimated NCO numbers to be of the same order as CO, ~10
294 events per meiosis, with gene conversion tracts ranging between a few tens to a few hundreds
295 of bp [19,20,50,51]. Notwithstanding this (surprisingly) low number of NCO, numbers of CO are
296 in agreement with chiasmata counting and immunolocalisation of CO markers. Thus, given the
297 200-300 DSB per meiosis in the these cells, the repair of at least 90% (and very possibly >98%
298 [52] of meiotic DSB in Arabidopsis is not accessible to analysis with current methods. In this
299 work, we present the development of meiotic prophase DNA synthesis labelling as a means to
300 fully characterise meiotic DSB-repair in Arabidopsis meiocytes.

301 Initial tests showed that incubating inflorescence stems for 24 hours in EdU solution
302 resulted in two clear sub-populations of meiocytes, distinguishable by their meiotic stage and
303 pattern of EdU labelling. The first consists of late G2 + early prophase I cells (leptotene,
304 zygotene) whose chromosomes show very strong EdU signals, either genome-wide or in large
305 patches. These patterns are consistent with those expected from pre-meiotic S-phase replicative
306 EdU incorporation:

307 I) This extensive EdU labelling is observed in meioses of both wild-type and *spo11* mutant
308 plants.

309 II) The extensive and intense fluorescent signals are similar to those observed in previous
310 reports of EdU/BrdU incorporation during pre-meiotic replication [11–13,29].

311 III) Extrapolating from published meiotic timelines and our own studies, PMC in pre-meiotic
312 S-phase at the beginning of the pulse are expected to advance at most to leptotene-
313 zygotene during the 24 hour EdU pulse (see Figure 1).

314 IV) The signal in partially labelled early prophase I cells corresponds principally to late-
315 replicating, DAPI-dense, heterochromatic regions, in accordance to expectations for cells in
316 late S-phase at the beginning of the EdU pulse.

317 The second population of EdU-labelled meiocytes includes cells at meiotic stages from
318 pachytene to the end of meiosis (tetrads), whose chromosomes show much fainter, discrete EdU
319 labelling. Clearly resolving into individual foci at the stages in which the chromosomes are less
320 condensed, these foci group into "patches" as chromosome condensation proceeds post-
321 prophase I. These foci have a number of characteristics which permit their identification with
322 confidence as meiotic DSB repair-associated DNA synthesis tracts:

323 I) These discrete EdU-label foci are SPO11-dependent, analogously to earlier observations in
324 yeast [9], confirming with high confidence that they result from EdU incorporation at DNA
325 synthesis tracts associated to meiotic DSB repair. Some EdU foci are observed in *spo11-1*
326 meioses, although at considerably lower numbers than in the wild type (39 versus 410 per
327 meiosis respectively). While some of these may come from mistaken assignation of organellar
328 DNA foci, we note that some crossing-over is detected in Arabidopsis *spo11* plants, RAD51 foci
329 are detected in Arabidopsis *spo11* meiosis and DMC1 foci in rice meioses [37,53–55].
330 Furthermore, given that both meiotic Arabidopsis SPO11 proteins are needed for normal meiotic
331 DSB induction, some leakage may occur in plants lacking one or the two SPO11 proteins [54,56–
332 59]. Alternatively, they may correspond to SPO11-independent breakage of mechanical,

333 chemical or enzymatic origin. If so, that they do produce DNA neo-synthesis tracts argues for
334 their repair by HR rather than End Joining.

335 II) The SPO11-dependent foci are seen at later meiotic stages than those with replicative
336 labelling and these nuclei had thus completed S-phase prior to the beginning of the pulse. Given
337 the known timing of meiosis in these cells, meiotic DSB repair DNA synthesis will have occurred
338 during the EdU pulse in these cells [9,13,14,38,60]. We note that while present in considerably
339 lower numbers than in the wild type (39 versus 410 per meiosis, respectively), there are some
340 EdU foci in *spo11-1* meioses.

341 III) The discrete EdU foci observed at pachytene and later stages are both much less intense
342 and smaller in size than the generalised labelling in leptotene-zygotene nuclei. This is expected
343 given the predicted size of DNA synthesis tracts associated to recombination events (few bases
344 to some kilobases of DNA), with respect to replicative labelling (megabases to the full genome).

345 IV) The numbers of EdU foci measured at pachytene concord with published estimations of
346 numbers of meiotic DSB and HR intermediates in Arabidopsis. A mean of 409.5 ± 7.96 (mean ±
347 SEM; n = 45 meioses) DNA repair-associated DNA synthesis foci were observed in WT
348 pachytenes. This number is a little higher than estimations of meiotic DSB numbers through
349 immunolocalisation of early recombination proteins in Arabidopsis (RAD51 in most cases).
350 Reported numbers of RAD51 foci per Arabidopsis meiosis range from 90 to 250 per meiosis, and
351 compare well with a recent report of 239 ± 30 (mean ± SD) prophase I SPO11-1 foci [56]. Given
352 the limitations of immunodetection and that the recruitment/release of these proteins at
353 DSB/recombination sites is dynamic, these numbers presumably under-estimate the true values.
354 Notably, a recent report using a STED super-resolution microscope found more than 1000 RAD51

355 foci per PMC meiosis [52]. Thus, the mean of 409.5 DNA repair-associated synthesis tracts per
356 meiosis reported here is probably closer to the true value than that of protein-immunodetection
357 approaches. It is of course necessary to take into account the fact that resolution of dHJ
358 recombination intermediates is expected to result in patches of neo-synthesized DNA on both
359 implicated chromatids, resulting in two foci from a single recombination event. Such events are
360 however estimated to represent ~5% or less of meiotic DSB repair events in Arabidopsis and so
361 are not expected to impact significantly the estimations of total events.

362 V) DAPI-dense heterochromatic, centromeric regions have a visibly lower density of SPO11-
363 dependent EdU foci in pachytene/diplotene and beyond (particularly noticeable at
364 diakinesis/MI). This concords with SPO11-oligo mapping of meiotic DSB patterns in Arabidopsis
365 PMC, which shows that centromeric regions have a much lower density of DSB than the rest of
366 the chromosome [34,36] .

367 VI) Combining labelling of EdU tracts with immunolocalization of MLH1 confirms that, as
368 expected, Class I CO are physically associated with the prophase I DSB repair DNA synthesis tracts
369 (Figure 6).

370

371 **Meiotic DSB repair-associated DNA synthesis tracts mirror meiotic recombination features**

372 As presented in Figure 7, different mechanisms of recombinational repair of meiotic DSB will
373 result in different patterns of DNA synthesis tracts associated to an HR event. The most obvious
374 difference is that DNA synthesis is expected to be found on only the recipient chromatid, which
375 carried the initiating DSB (Figure 7f), or on both the recipient and donor chromatids (Figure 7g,

376 h). SDSA and dHJ dissolution mechanisms would lea d to the former and dHJ resolution to the
377 latter. A special case is the BIR mechanism, which is expected to result in a long DNA synthesis
378 tract, potentially extending all the way to the end of the recipient chromatid (Figure 7c).

379 Visual inspection of the pachytene images clearly shows different configurations of the EdU
380 foci, which we have arbitrarily divided into 3 classes suggestive of the DNA synthesis patterns
381 expected at sites of recombination:

382 Class (1) isolated individual foci located on one of the two homologues (one lateral axis) (Fig.
383 5b, Fig. S2). Only the initially broken chromatid (recipient) will bear (EdU-substituted)
384 neosynthesized DNA tracts in repair via SDSA (Fig. 7a, b, f) and dHJ dissolution (Fig. 7a, d, e, f)
385 recombination.

386 Resolution of double Holiday junction (dHJ) intermediates (Fig7d) can give rise to gene
387 conversions, accompanied (Fig. 7g) or not (Fig. 7h) by a CO. In both cases, this can lead to the
388 presence of neo-synthesized DNA on both the donor and recipient chromatids. These events
389 would thus be expected to result in paired DNA synthesis tracts on the two participating
390 chromatids: either on one chromosome (Class (2) - one lateral axis) for sister chromatid events,
391 or on both homologues (Class (3) - both lateral axes).

392 Class (2) are thus "pairs" of foci on one of the two homologues (one SC lateral axis), which
393 could result from recombination between sister chromatids through the dHJ resolution pathway.

394 Class (3) are "pairs" of foci on the two homologues (both lateral axes), which could result
395 from recombination between homologues through the dHJ resolution pathway.

396

397 We find no evidence for long DNA synthesis tracts indicative of BIR recombination in our
398 images. Thus, either BIR replication tracts are not distinguishably longer than other DSB repair-
399 DNA synthesis, or the BIR mechanism is a minor (or non-) contributor to DSB repair in
400 Arabidopsis meiosis. In this context, we note that an earlier effort to detect mitotic BIR repair in
401 bleomycin-treated *Vicia faba* root tips described asymetric interstitial G2-phase EdU labelling of
402 interstitial tandem-repeat regions, although no extended labelling tracts out to the end of the
403 chromatid were observed [61].

404

405 Inference of the recombination pathways underlying the 3 classes of foci of course remains
406 speculative in the absence of molecular analyses of the EdU tracts themselves. FISH on extended
407 DNA fibres was used in an earlier study in yeast to determine the lengths and positioning of
408 BrdU-substituted DNA synthesis tracts with respect to DSB hotspots [9]. They observed two main
409 classes of tracts: tracts that extended from the DSB towards only one side of the DSB and tracts
410 that extended on both sides. These two classes correspond to the tracts expected in single DNA
411 molecules that took part in CO events in the first case and NCO events via SDSA in the second,
412 which were further validated studying their dynamics in recombination mutants. We have
413 previously carried out DNA combing plus fibre FISH in Arabidopsis [62], but the lack of strong
414 meiotic DSB hotspots with a precisely localised DSB site complicates the possible use of this
415 approach in Arabidopsis meiosis. Rather, we are actively developing an approach based on the
416 direct detection of EdU-substituted DNA tracts by Nanopore sequencing. It is hoped that this
417 approach will permit unambiguous characterisation of the principal meiotic recombination
418 products and underlying mechanisms in Arabidopsis, as well as of more complex events.

419

420

421

422

423 ## Materials and Methods

424 ### Plant material and growing conditions

425 Standard conditions were used for growth of wild-type *A. thaliana Col-0* and *spo11*-1-2 [37]
426 plants. Seeds were sown on soil substrate (Klasmann-Deilmann GmbH TS3 FIN 416GF, Geeste,
427 Germany), stratified for 2-4 days at 4°C and grown in climate chambers at 23°C and 60% relative
428 humidity, under a daily cycle of 16 hours of light (110-140 µmol m^{-2} s^{-1}) and 8 hours of darkness.

429 ### Meiotic chromosome preparation by spreading

430 Meiosis was analysed following the chromosome spreading method of Ross et al. [63], with
431 minor modifications. Inflorescences were collected in 3:1 ethanol:glacial acetic acid fixative
432 solution and left overnight at room temperature. The fixative was then substituted with fresh
433 fixative solution and the tubes were transferred to 4°C. This step was repeated the following 2-3
434 days. At this point, fixed inflorescences can be stored at 4°C for further use or prepared for
435 microscopy.

436 A number of fixed inflorescences were selected, deposited in a glass dissection well with 3:1
437 fixative solution and dissected under a stereomicroscope into individual flower buds, discarding

438 open flowers and buds with pollen (yellow anthers). The flower buds were then washed 3 x 2
439 minutes in citrate buffer and the buffer replaced with 500 µl of digestion enzyme mix (0.3% w/v
440 cellulase from *Trichoderma* sp. (Sigma-Aldrich), 0.3% w/v pectolyase from *Aspergillus japonicus*
441 (Sigma) and 0.3% w/v cytohelicase from *Helix pomatia* (Duchefa Biochemie) in citrate buffer).
442 The flower buds were incubated in the digestion mix for 2 hours at 37°C and the digestion
443 stopped by adding a greater volume of ice-cold citrate buffer. The well was placed under the
444 stereomicroscope and a single flower bud with a small volume of liquid was transferred to a slide
445 with a Pasteur pipette. The flower bud was macerated with a needle, a 10µl drop of ice-cold 60%
446 glacial acetic acid was added and the slide incubated for one minute on a hot plate at 45°C while
447 gently moving the drop with a flat needle. After the incubation, an extra 10 µl of ice-cold 60%
448 glacial acetic acid were added, followed by 100 µl of 3:1 fixative - first circling and flooding the
449 drop and then mixing with the drop by vigorously pipetting the last microliters. The liquid was
450 drained by tilting the slide, which was then further washed with another 100 µl of 3:1 fixative,
451 drained and left to air dry at room temperature.

452 To visualize the chromosomes, the slides were stained in Vectashield antifade mounting
453 medium with 1.5 µg/ml DAPI (# H-1200, Vector Laboratories, Burlingame, CA, USA), by putting a
454 drop on a coverslip which was then placed on a slide and gently squashed by thumb pressure.
455 Spreads were analysed with a Zeiss AxioImager Z1 microscope with a 100×/1.40 Oil Plan-
456 Apochromat objective and the Zeiss ZEN2Blue software (Carl Zeiss GmbH)in the channel for blue
457 fluorescence (Zeiss #49 HE filter).

458 EdU labelling and cytological detection

459 Among the different thymidine analogues commonly used to label *in vivo* DNA synthesis, 5-
460 Ethynyl-2'-deoxyuridine (EdU) has a number of advantages and has been preferred by the
461 Arabidopsis community in recent studies labelling DNA synthesis [12,29,30,64–67]. EdU can be
462 detected in intact double-strand DNA and this antibody-free technique simplifies the protocol
463 and offers better reproducibility.

464 EdU (#Ab146186, Abcam, UK) working solutions were prepared at 10mM in 1×PBS buffer.
465 Arabidopsis stems with apical inflorescences were submerged in water to avoid the introduction
466 of air bubbles (submerging only the stem segment to be cut, without wetting the inflorescences)
467 and cut obliquely 4-5cm below the inflorescence. Care was taken to make the cleanest cut
468 possible in order to avoid crushing vascular tissues. Open flowers and big leaves (if present) were
469 removed to avoid crowding the tube and minimize the risk of exhausting the solution due to
470 excessive transpiration. The inflorescences were incubated in 800µl of 10mM EdU in a 2ml
471 eppendorf tube for 24 hours, under the same growing conditions as the plants. To avoid tight
472 packing, a maximum of four or five inflorescence stems were incubated in one tube. After 24
473 hours the inflorescences were removed from the EdU solution and fixed in 3:1 ethanol:glacial
474 acetic acid solution.

475 Chromosome spreads were prepared as previously described and visualised under the
476 microscope to identify those slides with meiocytes at the desired meiotic stages. The slides were
477 first incubated in 4T (4×SSC, 0.5% v/v Tween 20) in a Coplin jar until the coverslips detached,
478 followed by 30' without coverslips in fresh 4T. The Click-iT reaction mix (Invitrogen Click-iT plus

479 Alexa-fluor 647 kit, Thermo-Fisher Scientific) to label EdU with the fluorochrome was prepared
480 following the manufacturer's instructions. Before labelling, the slides were washed for 5 minutes
481 with 1×PBS. A 30µl drop of Click-iT reagent was placed on a 32x24mm piece of parafilm and the
482 inverted slides were placed on top of the mix on the parafilm. The slides were incubated with the
483 mix for 30 minutes at 37°C in a dark moist chamber, washed for 5 minutes with 1×PBS in a Coplin
484 jar in the dark and mounted in Vectashield + DAPI for microscopy.

485 Pictures were taken using a Zeiss LSM800 confocal microscope applying the Airyscan
486 module and selecting the presets for each specific dye. EdU foci were quantified semi-
487 automatically using the IMARIS software *Spots* tool (Bitplane AG, Oxford Instruments, UK),
488 adding intensity filters for both channels to specifically selected visually detectable EdU foci that
489 co-localised with the DAPI fluorescence of the chromosomes. To analyze the chromatin and EdU
490 signal ultrastructure, we applied super-resolution spatial structured illumination microscopy (3D-
491 SIM) using a 63×/1.40 Oil Plan-Apochromat objective of an Elyra PS.1 microscope system and the
492 ZENBlack software (Carl Zeiss GmbH) [68]. Maximum intensity projections were calculated from
493 3D-SIM image stacks. Zoom-in sections were presented as single slices to indicate the subnuclear
494 chromatin structures at the super-resolution level.

495 Detection of MLH1 and EdU

496 For the detection of MLH1 and neo-synthesized DNA tracts with incorporated EdU, the
497 protocol for the immunolocalization of MLH1 [69] was adapted to include the Click-iT EdU
498 labelling. Chromosome spreads were prepared as previously described and visualized under the
499 microscope to identify those slides with meiocytes at the desired stages. The slides were

500 incubated in a Coplin jar with 100% ethanol to detach the coverslip and washed with 1×PBST
501 (0.1% Triton X-100 in 1×PBS. Another glass staining jar was filled with tri-sodium citrate buffer
502 pH7 and heated to boiling point in a microwave. The slides were placed in the heated tri-sodium
503 citrate solution for 45 seconds, after which they were returned to room temperature 1×PBST.

504 The rabbit anti-MLH1 primary antibodies (kindly provided by Mathilde Grelon, INRAe
505 Versailles [38]) was prepared at 1/200 in 1×PBST + 1% BSA. A 45µl drop was placed on a
506 32x24mm piece of parafilm and the inverted slide place on this. The slides were incubated for 2
507 days at 4°C in a dark moist chamber, after which they were washed 3 x 5 minutes with 1×PBST.
508 The secondary antibodies (goat anti-rabbit Alexa fluor 488) was prepared at 1/100 1×in PBST +
509 1% BSA, and 45µl were used per slide. Slides were incubated 30 minutes at 37°C in a dark moist
510 chamber, after which they were washed 2 x 5 minutes in 1×PBST, followed by one wash with
511 1×PBS. The Click-iT reaction was then performed as described above and the slide was mounted
512 in Vectashield + DAPI mounting medium for microscopy. Counting of MLH1 foci and co-
513 localization with EdU foci was carried out by visual inspection of images taken using the Zeiss
514 LSM800 confocal microscope plus the Airyscan module.

515

516

517

Acknowledgements

We thank the members of the recombination group and especially Olivier Da Ines, Jérémy Verbeke and Floriane Chéron for their help and suggestions. Mathilde Grelon kindly sent us the anti-MLH1 antiserum.

This work was supported by a European Marie Sklodowska Curie Actions Innovative Training Network grant (EU H2020-MSCA-ITN-2017-765212) to CIW, the Centre National de Recherche Scientifique (CNRS), the Institut National de la Santé et de la Recherche Médicale (Inserm) and the Université Clermont Auvergne. The funders had no role in study design, data collection and analysis, decision to publish, or preparation of the manuscript.

529

530 ## References

531 1. Arter M, Keeney S. Divergence and conservation of the meiotic recombination machinery.
532 Nat Rev Genet. 2023 [cited 6 Feb 2024]. doi:10.1038/s41576-023-00669-8

533 2. Hotta Y, Stern H. Transient phosphorylation of deoxyribosides and regulation of
534 deoxyribonucleic acid synthesis. J Biophys Biochem Cytol. 1961/11/01 ed. 1961;11: 311–9.
535 doi:10.1083/jcb.11.2.311

536 3. Lima-De-Faria A, German J, Ghatnekar M, McGovern J, Anderson L. In vitro labelling of
537 human meiotic chromosomes with H3-thymidine. Hereditas. 1968;60: 249–261.
538 doi:10.1111/j.1601-5223.1968.tb02205.x

539 4. Mukherjee AB, Cohen MM. DNA Synthesis during Meiotic Prophase in Male Mice. Nature.
540 1968;219: 489–490. doi:10.1038/219489a0

541 5. Prensky W. Uptake of thymine-methy6H3 by pachytene chromosomes of Lilium
542 longiflorum. Genetics. 1962;47: 977.

543 6. Wimber DE, Prensky W. Autoradiography with Meiotic Chromosomes of the Male Newt
544 (Triturus Viridescens) Using H3-Thymidine. Genetics. 1963/12/01 ed. 1963;48: 1731–8.
545 doi:10.1093/genetics/48.12.1731

546 7. Carpenter AT. EM autoradiographic evidence that DNA synthesis occurs at recombination
547 nodules during meiosis in Drosophila melanogaster females. Chromosoma. 1981/01/01 ed.
548 1981;83: 59–80. doi:10.1007/BF00286016

549 8. Moses MJ, Dresser ME, Poorman PA. Composition and role of the synaptonemal complex.
550 Symp Soc Exp Biol. 1984/01/01 ed. 1984;38: 245–70.

551 9. Terasawa M, Ogawa H, Tsukamoto Y, Shinohara M, Shirahige K, Kleckner N, et al. Meiotic
552 recombination-related DNA synthesis and its implications for cross-over and non-cross-
553 over recombinant formation. Proc Natl Acad Sci U S A. 2007/03/27 ed. 2007;104: 5965–70.
554 doi:10.1073/pnas.0611490104

555 10. Loidl J, Lukaszewicz A, Howard-Till RA, Koestler T. The Tetrahymena meiotic chromosome
556 bouquet is organized by centromeres and promotes interhomolog recombination. J Cell
557 Sci. 2012/09/15 ed. 2012;125: 5873–80. doi:10.1242/jcs.112664

558 11. Armstrong SJ, Franklin FCH, Jones GH. A meiotic time-course for Arabidopsis thaliana. Sex
559 Plant Reprod. 2003;16: 141–149. doi:10.1007/s00497-003-0186-4

560 12. Stronghill PE, Azimi W, Hasenkampf CA. A novel method to follow meiotic progression in
561 Arabidopsis using confocal microscopy and 5-ethynyl-2′-deoxyuridine labeling. Plant
562 Methods. 2014;10: 33. doi:10.1186/1746-4811-10-33

563 13. Sanchez-Moran E, Santos J-L, Jones GH, Franklin FCH. ASY1 mediates AtDMC1-dependent
564 interhomolog recombination during meiosis in Arabidopsis. Gene Dev. 2007;21: 2220–
565 2233. doi:10.1101/gad.439007

566 14. Allers T, Lichten M. Differential Timing and Control of Noncrossover and Crossover
567 Recombination during Meiosis. Cell. 2001;106: 47–57. doi:10.1016/s0092-8674(01)00416-
568 0

569 15. Börner GV, Hochwagen A, MacQueen AJ. Meiosis in budding yeast. Rothstein R, editor.

570 GENETICS. 2023;225: iyad125. doi:10.1093/genetics/iyad125

571 16. Collins I, Newlon CS. Meiosis-specific formation of joint DNA molecules containing
572 sequences from homologous chromosomes. Cell. 1994;76: 65–75. doi:10.1016/0092-
573 8674(94)90173-2

574 17. Hunter N, Kleckner N. The Single-End Invasion: An Asymmetric Intermediate at the Double-
575 Strand Break to Double-Holliday Junction Transition of Meiotic Recombination. Cell.
576 2001;106: 59–70. doi:10.1016/S0092-8674(01)00430-5

577 18. Schwacha A, Kleckner N. Identification of joint molecules that form frequently between
578 homologs but rarely between sister chromatids during yeast meiosis. Cell. 1994;76: 51–63.
579 doi:10.1016/0092-8674(94)90172-4

580 19. Wijnker E, James GV, Ding J, Becker F, Klasen JR, Rawat V, et al. The genomic landscape of
581 meiotic crossovers and gene conversions in Arabidopsis thaliana. eLife. 2013;2: e01426.
582 doi:10.7554/elife.01426

583 20. Lu P, Han X, Qi J, Yang J, Wijeratne AJ, Li T, et al. Analysis of Arabidopsis genome-wide
584 variations before and after meiosis and meiotic recombination by resequencing Landsberg
585 erecta and all four products of a single meiosis. 2012;22: 508–518.
586 doi:10.1101/gr.127522.111

587 21. Li R, Bitoun E, Altemose N, Davies RW, Davies B, Myers SR. A high-resolution map of non-
588 crossover events reveals impacts of genetic diversity on mammalian meiotic
589 recombination. Nat Commun. 2019;10: 3900. doi:10.1038/s41467-019-11675-y

590 22. Serrentino M-EM, Borde VV. The spatial regulation of meiotic recombination hotspots: are

591 all DSB hotspots crossover hotspots? Experimental cell research. 2012;318: 1347–1352.
592 doi:10.1016/j.yexcr.2012.03.025

593 23. Chakraborty P, Pankajam AV, Lin G, Dutta A, Krishnaprasad GN, Tekkedil MM, et al.
594 Modulating Crossover Frequency and Interference for Obligate Crossovers in
595 Saccharomyces cerevisiae Meiosis. G3 (Bethesda). 2017;7: 1511–1524.
596 doi:10.1534/g3.117.040071

597 24. Mancera E, Bourgon R, Brozzi A, Huber W, Steinmetz LM. High-resolution mapping of
598 meiotic crossovers and non-crossovers in yeast. Nature. 2008;454: 479–485.
599 doi:10.1038/nature07135

600 25. Valuchova S, Mikulkova P, Pecinkova J, Klimova J, Krumnikl M, Bainar P, et al. Imaging plant
601 germline differentiation within Arabidopsis flowers by light sheet microscopy. eLife.
602 2020;9: 3645–19. doi:10.7554/elife.52546

603 26. Rossig C, Lievre LL, Pilkington SM, Brownfield L. A simple and rapid method for imaging
604 male meiotic cells in anthers of model and non-model plant species. Plant Reprod.
605 2021;34: 37–46. doi:10.1007/s00497-021-00404-5

606 27. Prusicki MA, Keizer EM, Rosmalen RP van, Komaki S, Seifert F, Müller K, et al. Live cell
607 imaging of meiosis in Arabidopsis thaliana. eLife. 2019;8: e42834. doi:10.7554/elife.42834

608 28. Kurzbauer M-T, Uanschou C, Chen D, Schlögelhofer P. The recombinases DMC1 and RAD51
609 are functionally and spatially separated during meiosis in Arabidopsis. Plant Cell. 2012;24:
610 2058–2070. doi:10.1105/tpc.112.098459

611 29. Singh G, Da Ines O, Gallego ME, White CI. Analysis of the impact of the absence of RAD51

612 strand exchange activity in Arabidopsis meiosis. PLoS ONE. 2017;12: e0183006-16.
613 doi:10.1371/journal.pone.0183006

614 30. Varas J, Graumann K, Osman K, Pradillo M, Evans DE, Santos JL, et al. Absence of SUN1 and
615 SUN2 proteins in Arabidopsis thaliana leads to a delay in meiotic progression and defects in
616 synapsis and recombination. Plant J. 2015;81: 329–346. doi:10.1111/tpj.12730

617 31. Concia L, Brooks AM, Wheeler E, Zynda GJ, Wear EE, LeBlanc C, et al. Genome-Wide
618 Analysis of the Arabidopsis Replication Timing Program. PLANT PHYSIOLOGY. 2018;176:
619 2166–2185. doi:10.1104/pp.17.01537

620 32. Da Ines O, White CI. Centromere Associations in Meiotic Chromosome Pairing. Annual
621 review of genetics. 2015;49: 95–114. doi:10.1146/annurev-genet-112414-055107

622 33. Koornneef M, Fransz P, Jong H de. Cytogenetic tools for Arabidopsis thaliana. Chromosom
623 Res. 2003;11: 183–194. doi:10.1023/a:1022827624082

624 34. Naish M, Alonge M, Wlodzimierz P, Tock AJ, Abramson BW, Schmücker A, et al. The genetic
625 and epigenetic landscape of the Arabidopsis centromeres. Science. 2021;374: eabi7489.
626 doi:10.1126/science.abi7489

627 35. Rowan BA, Heavens D, Feuerborn TR, Tock AJ, Henderson IR, Weigel D. An Ultra High-
628 Density Arabidopsis thaliana Crossover Map That Refines the Influences of Structural
629 Variation and Epigenetic Features. Genetics. 2019;213: genetics.302406.2019.
630 doi:10.1534/genetics.119.302406

631 36. Choi K, Zhao X, Tock AJ, Lambing C, Underwood CJ, Hardcastle TJ, et al. Nucleosomes and
632 DNA methylation shape meiotic DSB frequency in Arabidopsis thaliana transposons and

633 gene regulatory regions. Genome research. 2018;28: 532–546. doi:10.1101/gr.225599.117

634 37. Grelon M, Vezon D, Gendrot G, Pelletier G. AtSPO11-1 is necessary for efficient meiotic
635 recombination in plants. EMBO J. 2001;20: 589–600. doi:10.1093/emboj/20.3.589

636 38. Chelysheva L, Grandont L, Vrielynck N, le Guin S, Mercier R, Grelon M. An Easy Protocol for
637 Studying Chromatin and Recombination Protein Dynamics during Arabidopsisthaliana
638 Meiosis: Immunodetection of Cohesins, Histones and MLH1. Cytogenetic and Genome
639 Research. 2010;129: 143–153. doi:10.1159/000314096

640 39. Schwacha A, Kleckner N. Interhomolog Bias during Meiotic Recombination: Meiotic
641 Functions Promote a Highly Differentiated Interhomolog-Only Pathway. Cell. 1997;90:
642 1123–1135. doi:10.1016/S0092-8674(00)80378-5

643 40. Goldfarb T, Lichten M. Frequent and efficient use of the sister chromatid for DNA double-
644 strand break repair during budding yeast meiosis. PLoS biology. 2010;8: e1000520.
645 doi:10.1371/journal.pbio.1000520

646 41. Oh SD, Lao JP, Hwang PY-H, Taylor AF, Smith GR, Hunter N. BLM Ortholog, Sgs1, Prevents
647 Aberrant Crossing-over by Suppressing Formation of Multichromatid Joint Molecules. Cell.
648 2007;130: 259–272. doi:10.1016/j.cell.2007.05.035

649 42. Oh SD, Lao JP, Taylor AF, Smith GR, Hunter N. RecQ Helicase, Sgs1, and XPF Family
650 Endonuclease, Mus81-Mms4, Resolve Aberrant Joint Molecules during Meiotic
651 Recombination. Molecular Cell. 2008;31: 324–336. doi:10.1016/j.molcel.2008.07.006

652 43. Jackson JA, Fink GR. Meiotic recombination between duplicated genetic elements in
653 Saccharomyces cerevisiae. Genetics. 1985;109: 303–332. doi:10.1093/genetics/109.2.303

654 44. Haber JE, Thorburn PC, Rogers D. Meiotic and mitotic behaviour of dicentric chromosomes
655 in Saccharomyces cerevisiae. Genetics. 1984;106: 185–205.
656 doi:10.1093/genetics/106.2.185

657 45. Webber HA, Howard L, Bickel SE. The cohesion protein ORD is required for homologue bias
658 during meiotic recombination. The Journal of Cell Biology. 2004;164: 819–829.
659 doi:10.1083/jcb.200310077

660 46. Cole F, Baudat F, Grey C, Keeney S, De Massy B, Jasin M. Mouse tetrad analysis provides
661 insights into recombination mechanisms and hotspot evolutionary dynamics. Nat Genet.
662 2014;46: 1072–1080. doi:10.1038/ng.3068

663 47. Almanzar DE, Gordon SG, Rog O. Meiotic sister chromatid exchanges are rare in C. elegans.
664 Current Biology. 2021;31: 1499-1507.e3. doi:10.1016/j.cub.2020.11.018

665 48. Toraason E, Horacek A, Clark C, Glover ML, Adler VL, Premkumar T, et al. Meiotic DNA
666 break repair can utilize homolog-independent chromatid templates in C. elegans. Current
667 Biology. 2021;31: 1508-1514.e5. doi:10.1016/j.cub.2021.03.008

668 49. Billmyre KK, Hughes SE. Meiosis: The elusive sister chromatid repair. Current Biology.
669 2021;31: R454–R456. doi:10.1016/j.cub.2021.03.093

670 50. Yang S, Yuan Y, Wang L, Li J, Wang W, Liu H, et al. Great majority of recombination events
671 in Arabidopsis are gene conversion events. Proceedings of the National Academy of
672 Sciences of the United States of America. 2012;109: 20992–20997.
673 doi:10.1073/pnas.1211827110

674 51. Drouaud J, Khademian H, Giraut L, Zanni V, Bellalou S, Henderson IR, et al. Contrasted

675 patterns of crossover and non-crossover at Arabidopsis thaliana meiotic recombination
676 hotspots. Hong Ma, editor. PLoS Genetics. 2013;9: e1003922.
677 doi:10.1371/journal.pgen.1003922

678 52. Sims J, Schlögelhofer P, Kurzbauer M-T. From Microscopy to Nanoscopy: Defining an
679 Arabidopsis thaliana Meiotic Atlas at the Nanometer Scale. Front Plant Sci. 2021;12:
680 672914. doi:10.3389/fpls.2021.672914

681 53. Fayos I, Meunier AC, Vernet A, Navarro-Sanz S, Portefaix M, Lartaud M, et al. Assessment
682 of the roles of SPO11-2 and SPO11-4 in meiosis in rice using CRISPR/Cas9 mutagenesis.
683 Journal of Experimental Botany. 2020;71: 7046–7058. doi:10.1093/jxb/eraa391

684 54. Stacey NJ, Kuromori T, Azumi Y, Roberts G, Breuer C, Wada T, et al. Arabidopsis SPO11-2
685 functions with SPO11-1 in meiotic recombination. The Plant Journal. 2006;48: 206–216.
686 doi:10.1111/j.1365-313X.2006.02867.x

687 55. Sims J, Copenhaver GP, Schlögelhofer P. Meiotic DNA Repair in the Nucleolus Employs a
688 Nonhomologous End-Joining Mechanism. The Plant Cell. 2019;31: 2259–2275.
689 doi:10.1105/tpc.19.00367

690 56. Vrielynck N, Schneider K, Rodriguez M, Sims J, Chambon A, Hurel A, et al. Conservation and
691 divergence of meiotic DNA double strand break forming mechanisms in Arabidopsis
692 thaliana. Nucleic Acids Res. 2021. doi:10.1093/nar/gkab715

693 57. Sprink T, Hartung F. Heterologous Complementation of SPO11-1 and -2 Depends on the
694 Splicing Pattern. IJMS. 2021;22: 9346. doi:10.3390/ijms22179346

695 58. Vrielynck N, Chambon A, Vezon D, Pereira L, Chelysheva L, Muyt AD, et al. A DNA

696 topoisomerase VI–like complex initiates meiotic recombination. Science (New York, NY).
697 2016;351: 939–943. doi:10.1126/science.aad5196

698 59. Hartung F, Wurz-Wildersinn R, Fuchs J, Schubert I, Suer S, Puchta H. The catalytically active
699 tyrosine residues of both SPO11-1 and SPO11-2 are required for meiotic double-strand
700 break induction in Arabidopsis. The Plant cell. 2007;19: 3090–3099.
701 doi:10.1105/tpc.107.054817

702 60. Alonso-Ramos P, Álvarez-Melo D, Strouhalova K, Pascual-Silva C, Garside GB, Arter M, et al.
703 The Cdc14 Phosphatase Controls Resolution of Recombination Intermediates and
704 Crossover Formation during Meiosis. Int J Mol Sci. 2021;22: 9811.
705 doi:10.3390/ijms22189811

706 61. Schubert I, Schubert V, Fuchs J. No Evidence for “Break-Induced Replication” in a Higher
707 Plant – But Break-Induced Conversion May Occur. Front Plant Sci. 2011;2: 8.
708 doi:10.3389/fpls.2011.00008

709 62. Vannier J-B, Depeiges A, White C, Gallego ME. Two roles for Rad50 in telomere
710 maintenance. The EMBO Journal. 2006;25: 4577–4585. doi:10.1038/sj.emboj.7601345

711 63. Ross KJ, Fransz P, Jones GH. A light microscopic atlas of meiosis in Arabidopsis thaliana.
712 Chromosom Res : Int J Mol, Supramol Evol Asp Chromosom Biol. 1996;4: 507–16.
713 doi:10.1007/bf02261778

714 64. Dvořáčková M, Raposo B, Matula P, Fuchs J, Schubert V, Peška V, et al. Replication of
715 ribosomal DNA in Arabidopsis occurs both inside and outside the nucleolus during S phase
716 progression. J Cell Sci. 2017;131: jcs202416. doi:10.1242/jcs.202416

717 65. Lambing C, Osman K, Nuntasoontorn K, West A, Higgins JD, Copenhaver GP, et al.
718 Arabidopsis PCH2 Mediates Meiotic Chromosome Remodeling and Maturation of
719 Crossovers. PLoS Genet. 2015;11: e1005372. doi:10.1371/journal.pgen.1005372

720 66. Vanstraelen M, Baloban M, Ines OD, Cultrone A, Lammens T, Boudolf V, et al. APC/C-
721 CCS52A complexes control meristem maintenance in the Arabidopsis root. Proceedings of
722 the National Academy of Sciences of the United States of America. 2009;106: 11806–
723 11811. doi:10.1073/pnas.0901193106

724 67. Amiard S, Charbonnel C, Allain E, Depeiges A, White CI, Gallego ME. Distinct roles of the
725 ATR kinase and the Mre11-Rad50-Nbs1 complex in the maintenance of chromosomal
726 stability in Arabidopsis. THE PLANT CELL. 2010;22: 3020–3033.
727 doi:10.1105/tpc.110.078527

728 68. Weisshart K, Fuchs J, Schubert V. Structured Illumination Microscopy (SIM) and
729 Photoactivated Localization Microscopy (PALM) to Analyze the Abundance and Distribution
730 of RNA Polymerase II Molecules on Flow-sorted Arabidopsis Nuclei. BIO-PROTOCOL.
731 2016;6. doi:10.21769/BioProtoc.1725

732 69. Chelysheva LA, Grandont L, Grelon M. Immunolocalization of Meiotic Proteins in
733 Brassicaceae: Method 1. In: Pawlowski WP, Grelon M, Armstrong S, editors. Plant Meiosis:
734 Methods and Protocols. Totowa, NJ: Humana Press; 2013. pp. 93–101. doi:10.1007/978-1-
735 62703-333-6_9

736

737

738 ## Figure Legends

739 **Figure 1. EdU labelling strategy and timeline of** Arabidopsis **male meiosis.** Pollen mother cell nuclei
740 were fixed and isolated at the end of a 24-hour pulse of EdU incorporporation. Cells which traversed all or
741 part of the pre-meiotic S-phase during the pulse will show replicative EdU incorporation and be at
742 G2/leptotene/zygotene stages at the end of the pulse, with some overlap into early pachytene. Fully
743 pachytene nuclei (mid-late pachytene) will not show replicative labeling, but will have traversed the
744 leptotene and zygotene stages in the presence of EdU. Any EdU incorporation in these (or later) nuclei
745 will be due to non-S-Phase DNA synthesis.
746
747 **Figure 2. DSB repair-associated DNA synthesis tracts are detected from pachytene up to the end of**
748 **meiosis.** a) Meiosis I and b) meiosis II stages in *A. thaliana* wildtype. S-phase, replicative DNA labelling is
749 seen at early G2/letotene and zygotene stages, while clear, discrete foci of EdU substituted DNA are
750 visible in the chromosomes at later stages from pachytene onwards. Rectangles indicate the enlarged
751 regions presented in the zooms. Non-chromosomal EdU foci correspond to labelling of mitochondrial
752 genome replication. 3µm scale bars are shown at the bottom left of each image (1µm for the zooms).
753 Images were taken with the confocal microscope + Airyscan module.
754
755 **Figure 3. DSB repair-associated DNA synthesis is SPO11- dependent.**
756 a) Meiosis I and b) meiosis II stages in *A. thaliana* spo11-1 mutants. As for WT meiosis (Figure 2),
757 replicative S-phase labelling is seen at early stages, corresponding to G2/leptotene and zygotene. As
758 expected, a striking reduction in numbers of EdU foci (compared to WT) is observed in spo11-1 mutants
759 at stages from mid-prophase I onwards (corresponding to pachytene and later stages). Rectangles

760 indicate the enlarged regions presented in the zooms. Images taken with the confocal microscope with
761 Airyscan module. 3µm scale bars are shown at the bottom left of each image (1µm for the zooms).

762 **Figure 4. Concordance of numbers of SPO11-dependent, meiotic DNA synthesis foci and estimated**
763 **DSB numbers.**

764 a) Representative images of wild-type pachytene and *spo11-1* pachytene-like meiotic stages. The merged
765 DAPI (blue) plus EdU (orange) images are accompanied by the computer-generated images of the scored
766 EdU foci (white, right panels). EdU foci colocalising with chromosome fibres were retained for counting
767 and mean intensity used to exclude the much-brighter organellar foci (see text). The Images taken with
768 the confocal microscope with Airyscan module. 3µm scale bars are shown at the bottom left of each
769 image. b) Numbers of EdU foci on the chromosomes quantified with Imaris software show clearly the
770 SPO11-dependence of these DNA synthesis tracts and that their numbers correspond to expectations
771 from DSB counting in PMC. The mean number of foci/nucleus and number of nuclei counted are shown
772 above the graph.

773

774 **Figure 5. Ultrastructure of SPO11-dependent, meiotic DNA synthesis foci on the synaptonemal**
775 **complex (SC) during pachytene.**

776 a) Expected configurations of DNA synthesis tracts resulting from different mechanisms of homologous
777 recombinational repair of meiotic DSB: Synthesis-Dependent Strand Annealing (SDSA), double-Holliday
778 Junction (dHJ), Gene Conversion ± Crossover (GC±CO) and Break-Induced Replication (BIR). b) Examples
779 of segments of pachytene SC. Isolated individual foci (one SC lateral axis, white circle) and pairs of foci on
780 one homologue (one SC lateral axis, green circle) or the two homologues (both SC lateral axes, yellow
781 circle) are highlighted. The images represent a single slice of 3D-SIM image stacks. 0.5µm scale bars are
782 shown at the bottom left of each image.

783 **Figure 6. Class I crossovers (CO) colocalize with prophase I DNA synthesis tracts**.

784 a) Wild-type pachytene cell showing DAPI staining (blue), prophase I DNA synthesis tracts (EdU, orange)
785 and Class 1 CO (MLH1, green). **b)** Examples of colocalising and adjacent MLH1 and EdU foci. The
786 quantification (right) shows that 95.6% of MLH1 foci co-localize with EdU tracts, and the remainder are
787 adjacent to one. a) is a confocal image and b) a single slice of a 3D-SIM image stack. Scale bars are 1µm in
788 (a) and 0.1µm in (b).
789
790 **Figure 7. Recombination mechanisms and DNA synthesis tracts.**
791 Following resection and invasion of the donor chromatid (a), DNA neo-synthesis tracts resulting from
792 repair of DSB are expected to be found only on the recipient chromatid in gene conversions (f) resulting
793 from SDSA (b) or dHJ dissolution (e) pathways. A special case of this is the BIR pathway (c), which will
794 result in a long synthesis tract, potentially extending all the way to the end of the recipient chromatid.
795 DNA synthesis tracts are expected to be found on both the recipient and donor chromatids in gene
796 conversions, associated (g) or not (h) to a CO, resulting from resolution of the dHJ intermediate (d).
797
798

799 Supplemental Figure Legends

800
801 **Figure S1. Discrete foci of EdU substituted DNA are visible in pachytene chromosomes of Arabidopsis**
802 **PMC.**
803 Examples of prophase I DNA labelling in pachtene nuclei of wildtype PMC. Each row is the same nucleus,
804 imaged with DAPI fluorescence (white, left), EdU (orange, middle) and the merged image (right). Images
805 taken with the confocal microscope with Airyscan module. 2µm scale bars are included at the bottom left
806 of each image.

807

808 **Figure S2. Distribution of SPO11-dependent, meiotic DNA synthesis foci on paired pachytene**

809 **chromosomes from two different cells.**

810 Zoomed regions from SIM (a) and Confocal (b) images of meiotic pachytenes, showing the distribution of

811 EdU-labelled meiotic prophase I DNA synthesis foci (a)red, b) orange) on the DAPI-stained chromosome

812 fibres (white) of the synaptonemal complexes. 0.5µm scale bars are included at the bottom left of each

813 image.

Figure 1

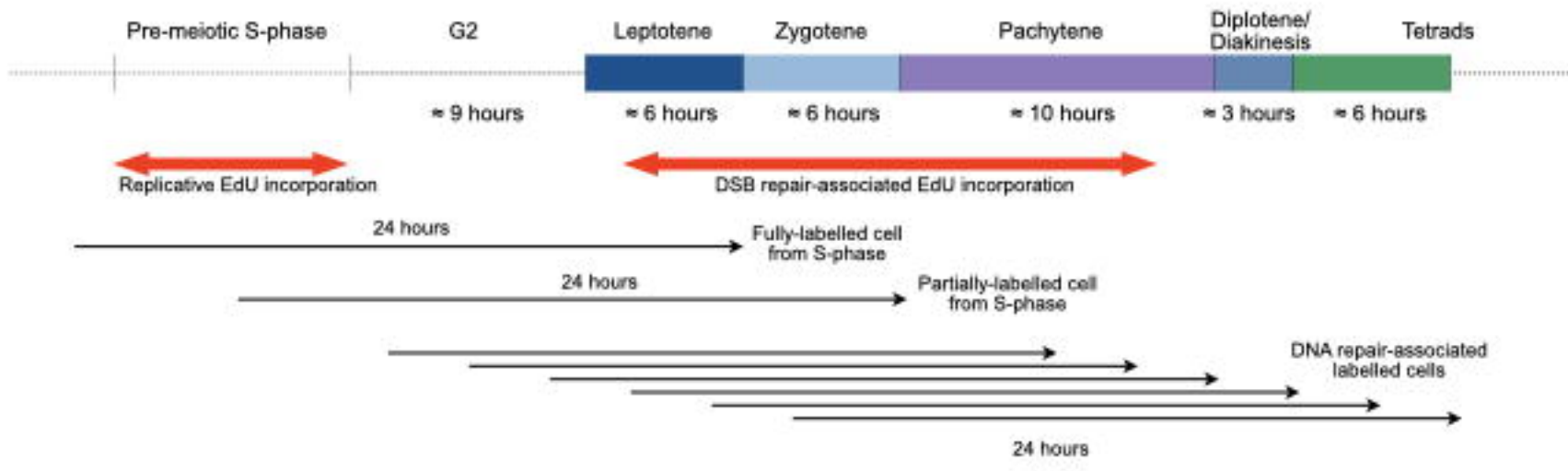

Figure 1. EdU labelling strategy and timeline of *Arabidopsis* male meiosis. Pollen mother cell nuclei were fixed and isolated at the end of a 24-hour pulse of EdU incorporporation. Cells which traversed all or part of the pre-meiotic S-phase during the pulse will show replicative EdU incorporation and be at G2/leptotene/zygotene stages at the end of the pulse, with some overlap into early pachytene. Fully pachytene nuclei (mid-late pachytene) will not show replicative labeling, but will have traversed the leptotene and zygotene stages in the presence of EdU. Any EdU incorporation in these (or later) nuclei will be due to non-S-Phase DNA synthesis.

Figure 2

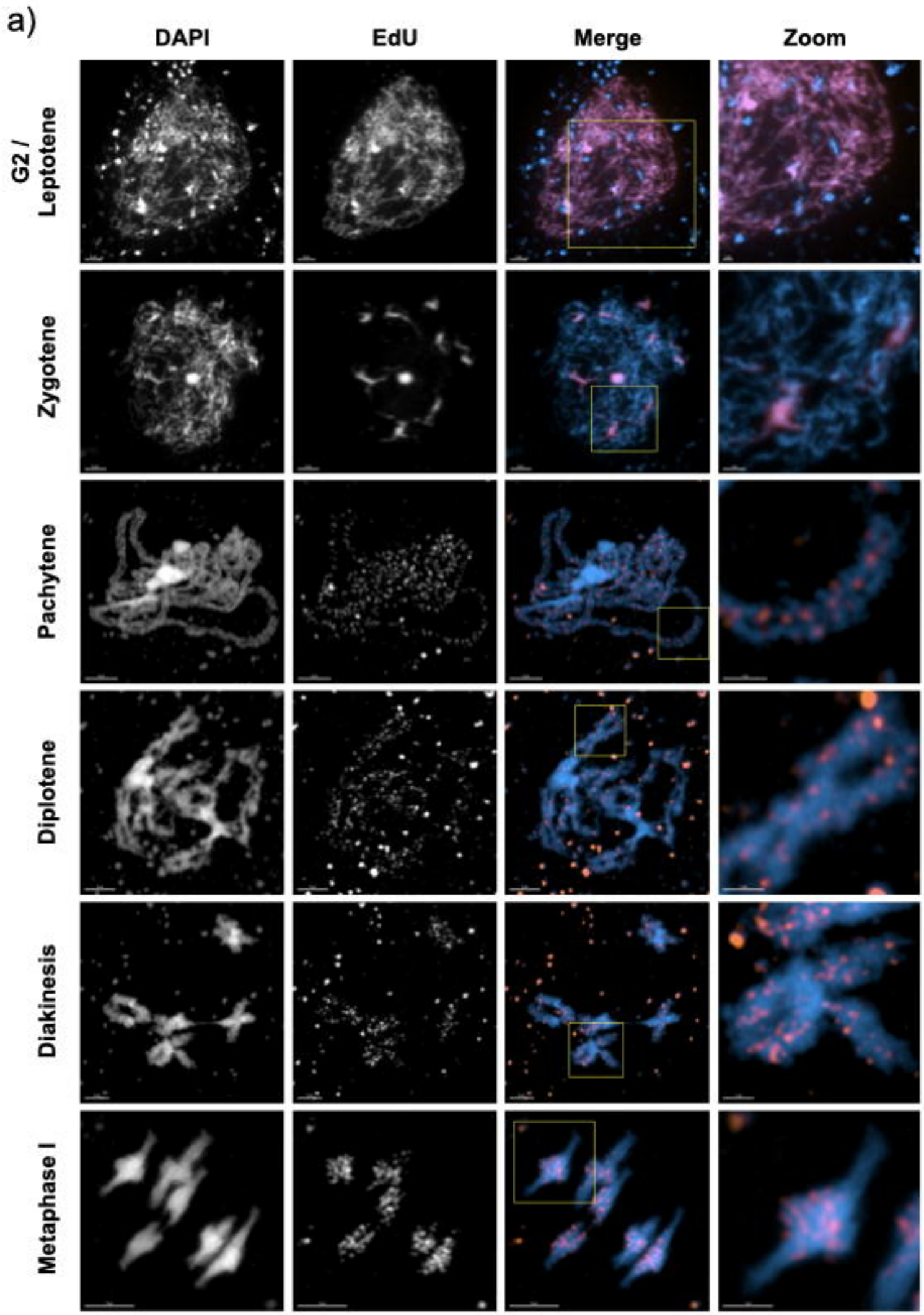
a)
DAPI
EdU
Merge
Zoom
G2 / Leptotene
Zygotene
Pachytene
Diplotene
Diakinesis
Metaphase I

Figure 2

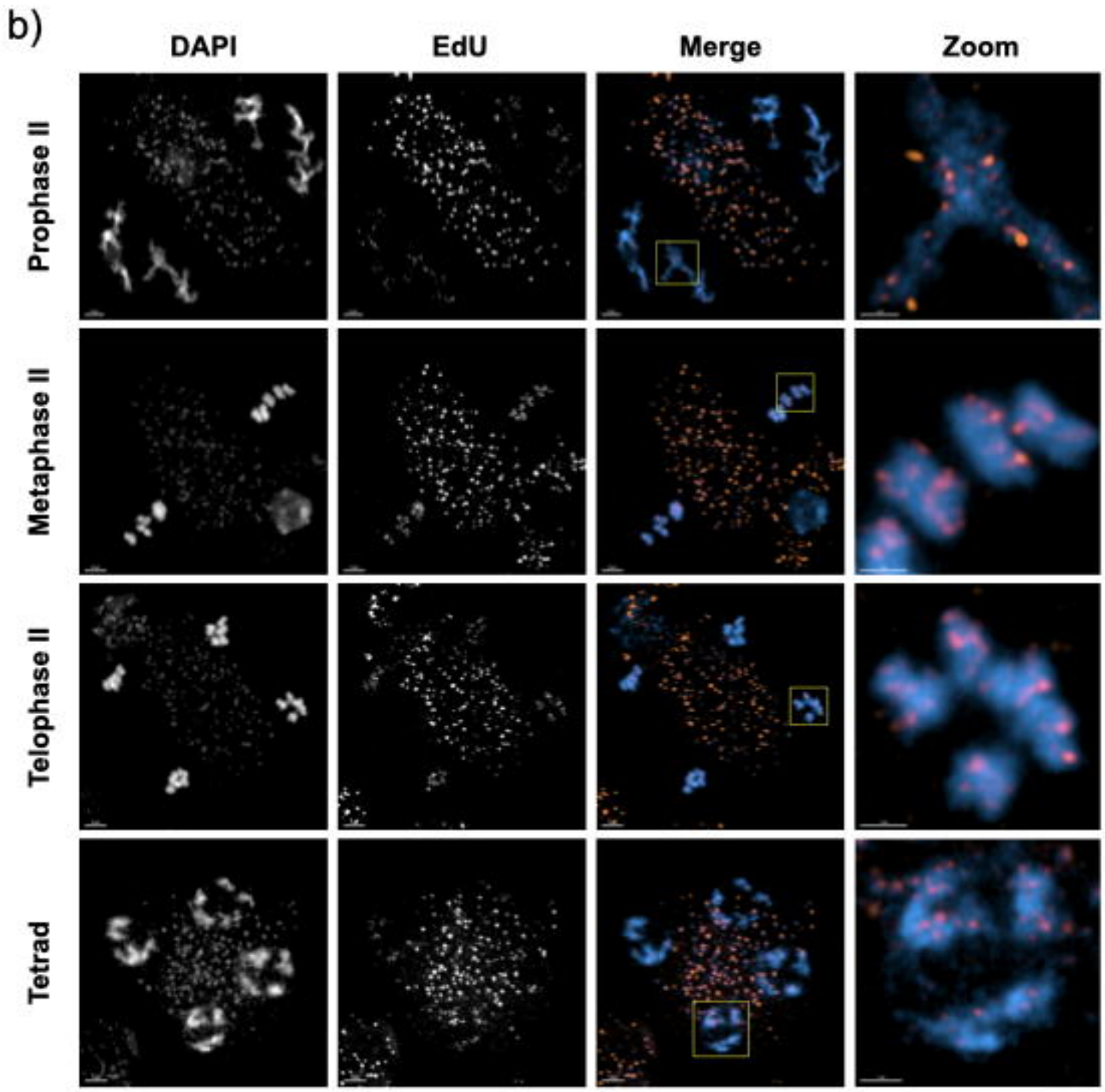

Figure 2. DSB repair-associated DNA synthesis tracts are detected from pachytene up to the end of meiosis. a) Meiosis I and b) meiosis II stages in *A. thaliana* wildtype. S-phase, replicative DNA labelling is seen at early G2/letotene and zygotene stages, while clear, discrete foci of EdU substituted DNA are visible in the chromosomes at later stages from pachytene onwards. Rectangles indicate the enlarged regions presented in the zooms. Non-chromosomal EdU foci correspond to labelling of mitochondrial genome replication. 3µm scale bars are shown at the bottom left of each image (1µm for the zooms). Images were taken with the confocal microscope + Airyscan module.

Figure 3

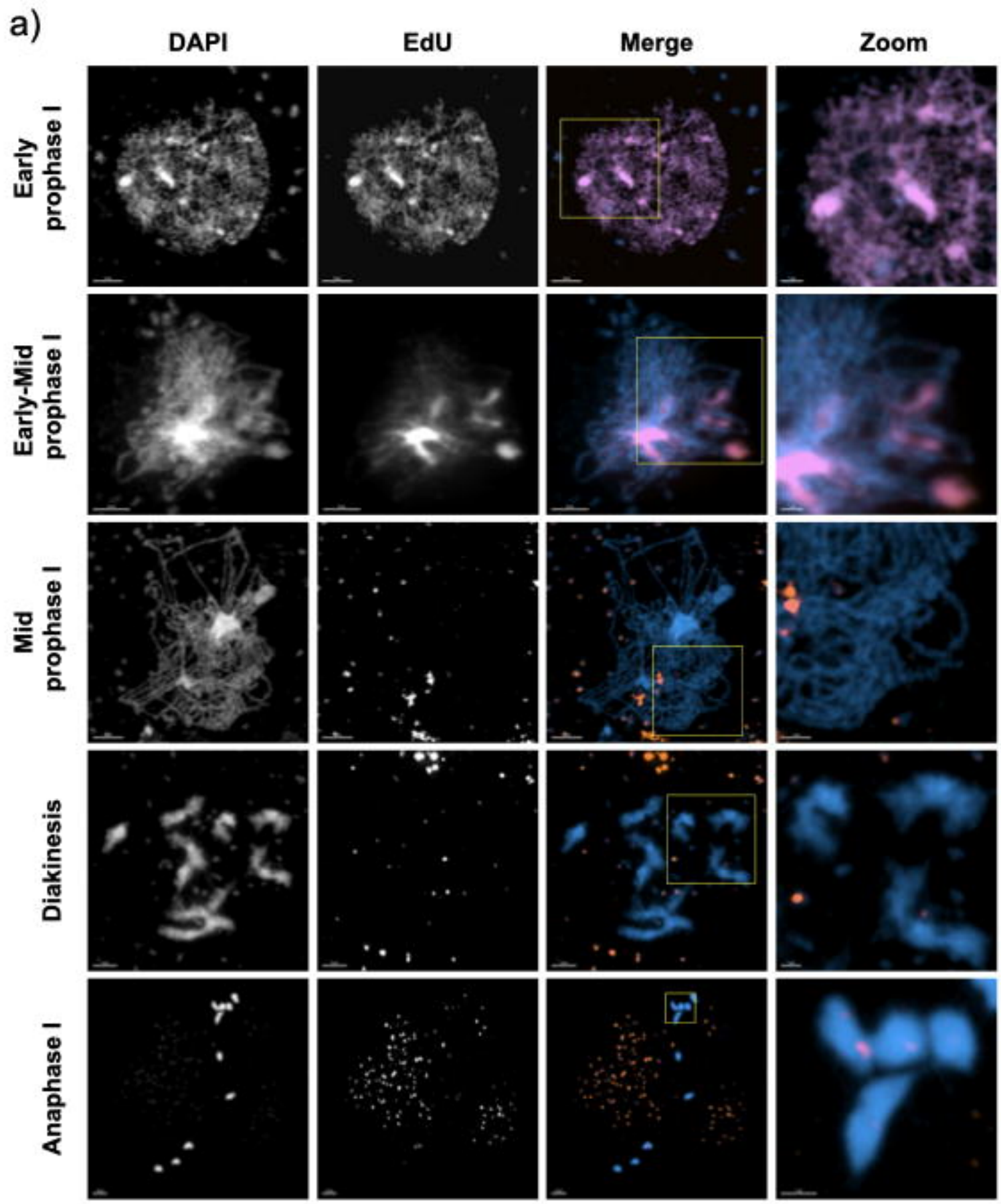
a)
DAPI
EdU
Merge
Zoom
Early prophase I
Early-Mid prophase I
Mid prophase I
Diakinesis
Anaphase I

Figure 3

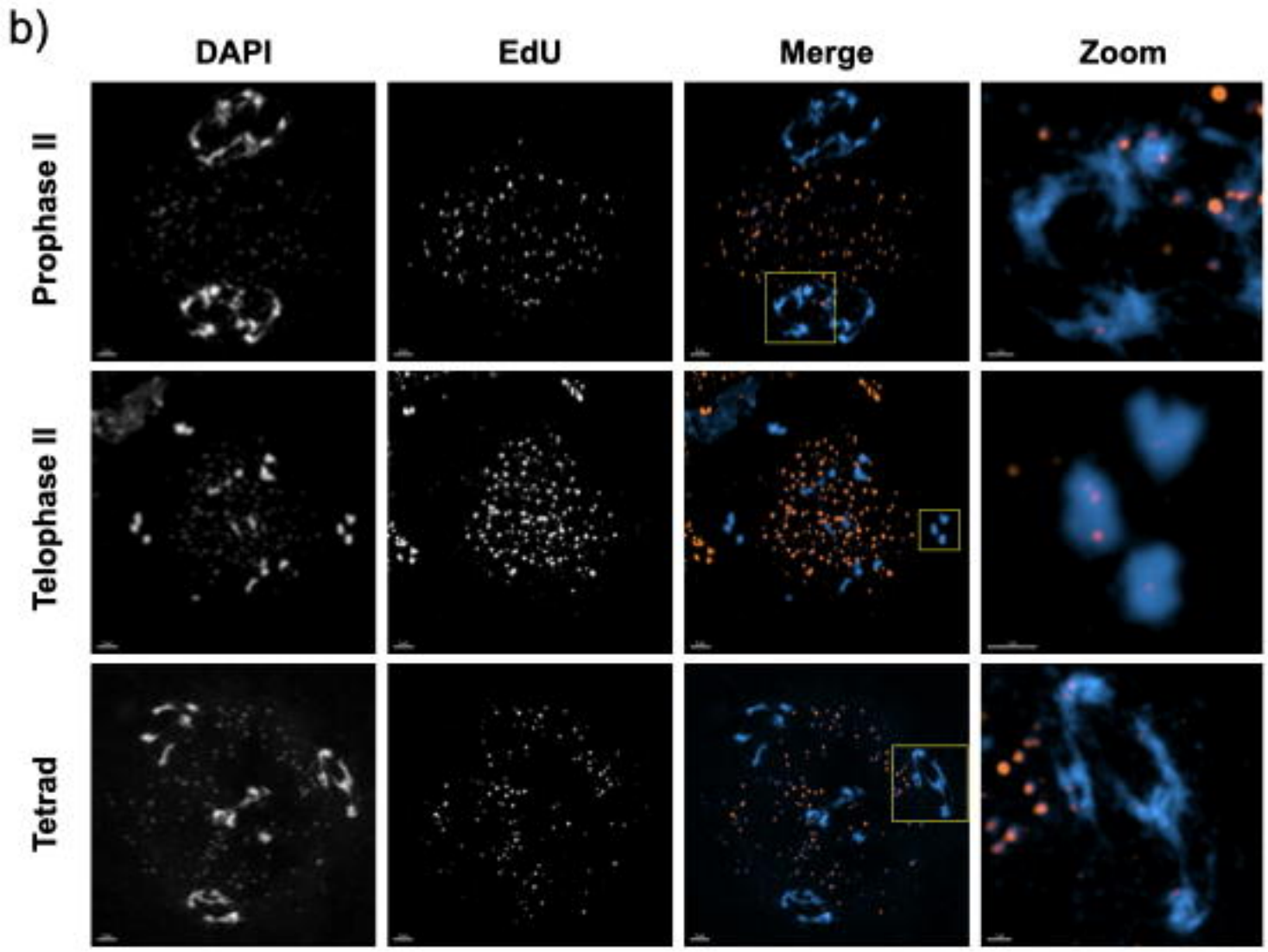

Figure 3. DSB repair-associated DNA synthesis is SPO11-dependent.
a) Meiosis I and b) meiosis II stages in *A. thaliana* spo11-1 mutants. As for WT meiosis (Figure 2), replicative S-phase labelling is seen at early stages, corresponding to G2/leptotene and zygotene. As expected, a striking reduction in numbers of EdU foci (compared to WT) is observed in spo11-1 mutants at stages from mid-prophase I onwards (corresponding to pachytene and later stages). Rectangles indicate the enlarged regions presented in the zooms. Images taken with the confocal microscope with Airyscan module. 3µm scale bars are shown at the bottom left of each image (1µm for the zooms).

Figure 4

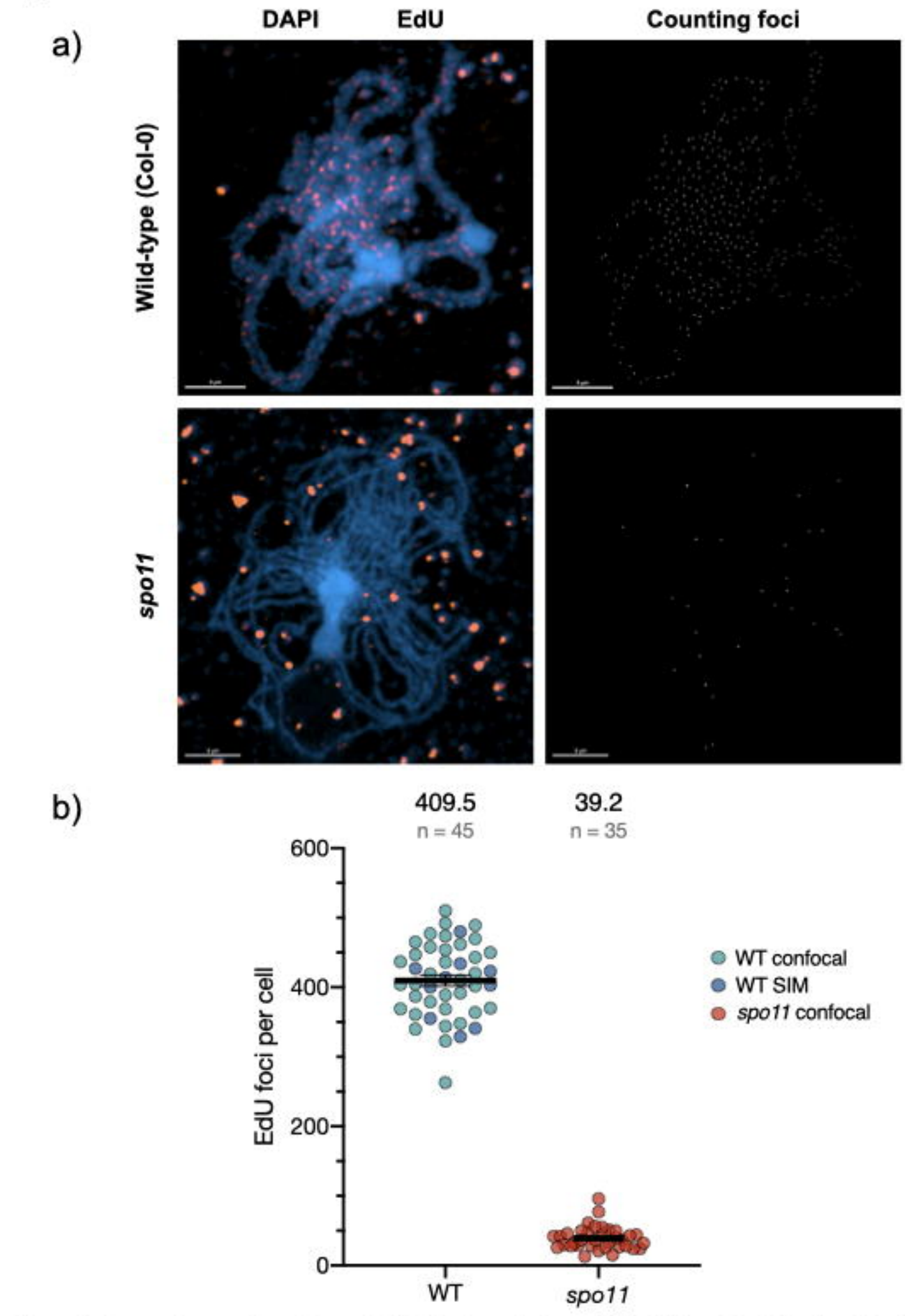

Figure 4. Concordance of numbers of SPO11-dependent, meiotic DNA synthesis foci and estimated DSB numbers. a) Representative images of wild-type pachytene and spo11-1 pachytene-like meiotic stages. The merged DAPI (blue) plus EdU (orange) images are accompanied by the computer-generated images of the scored EdU foci (white, right panels). EdU foci colocalising with chromosome fibres were retained for counting and mean intensity used to exclude the much-brighter organellar foci (see text). The Images taken with the confocal microscope with Airyscan module. 3µm scale bars are shown at the bottom left of each image. b) Numbers of EdU foci on the chromosomes quantified with Imaris software show clearly the SPO11-dependence of these DNA synthesis tracts and that their numbers correspond to expectations from DSB counting in PMC. The mean number of foci/nucleus and number of nuclei counted are shown above the graph.

Figure 5

a)

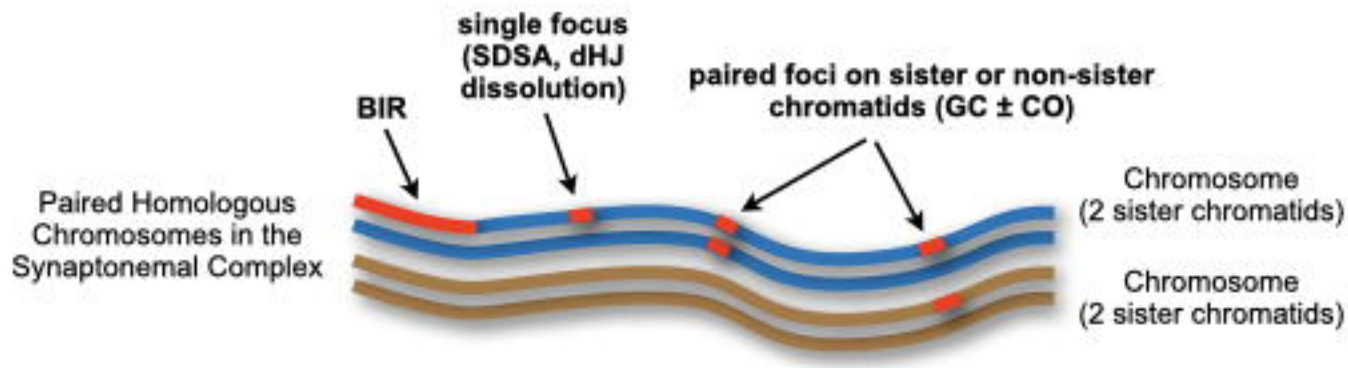

b)

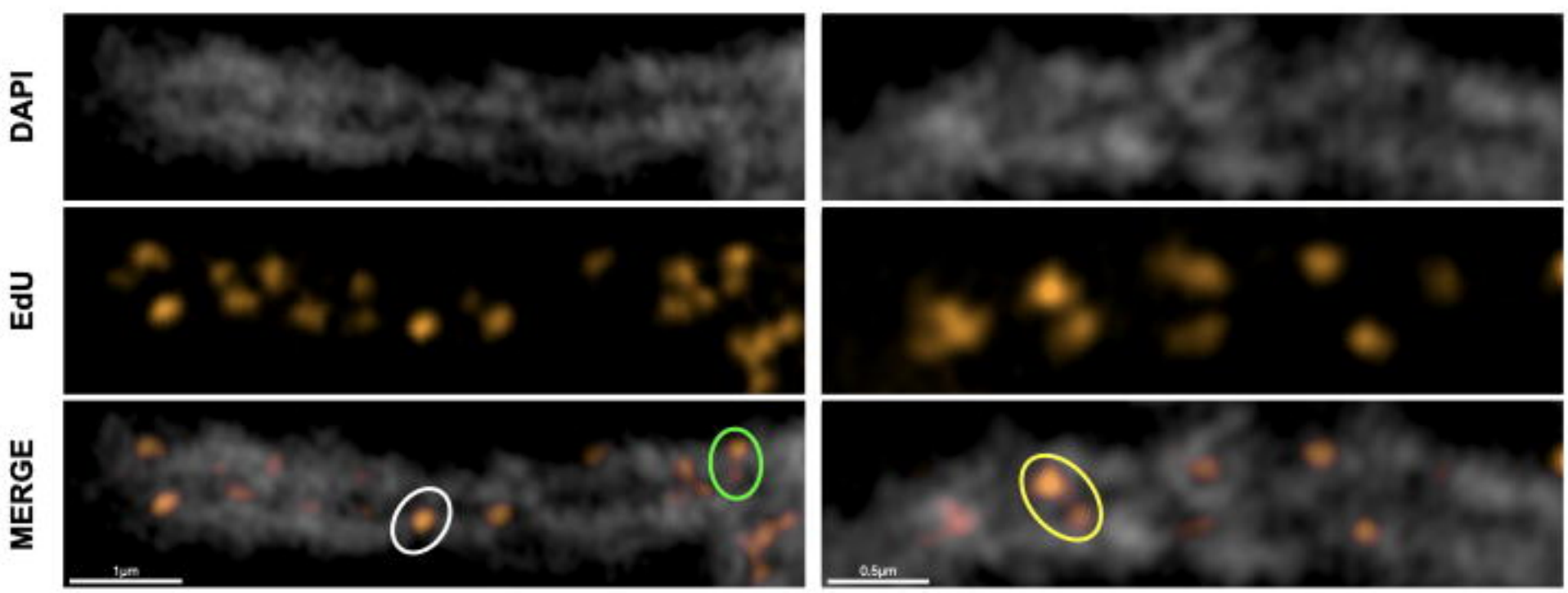

Figure 5. Ultrastructure of SPO11-dependent, meiotic DNA synthesis foci on the synaptonemal complex (SC) during pachytene. a) Expected configurations of DNA synthesis tracts resulting from different mechanisms of homologous recombinational repair of meiotic DSB: Synthesis-Dependent Strand Annealing (SDSA), double-Holliday Junction (dHJ), Gene Conversion ± Crossover (GC±CO) and Break-Induced Replication (BIR). b) Examples of segments of pachytene SC. Isolated individual foci (one SC lateral axis, white circle) and pairs of foci on one homologue (one SC lateral axis, green circle) or the two homologues (both SC lateral axes, yellow circle) are highlighted. The images represent a single slice of 3D-SIM image stacks. 0.5µm scale bars are shown at the bottom left of each image.

Figure 6

a)

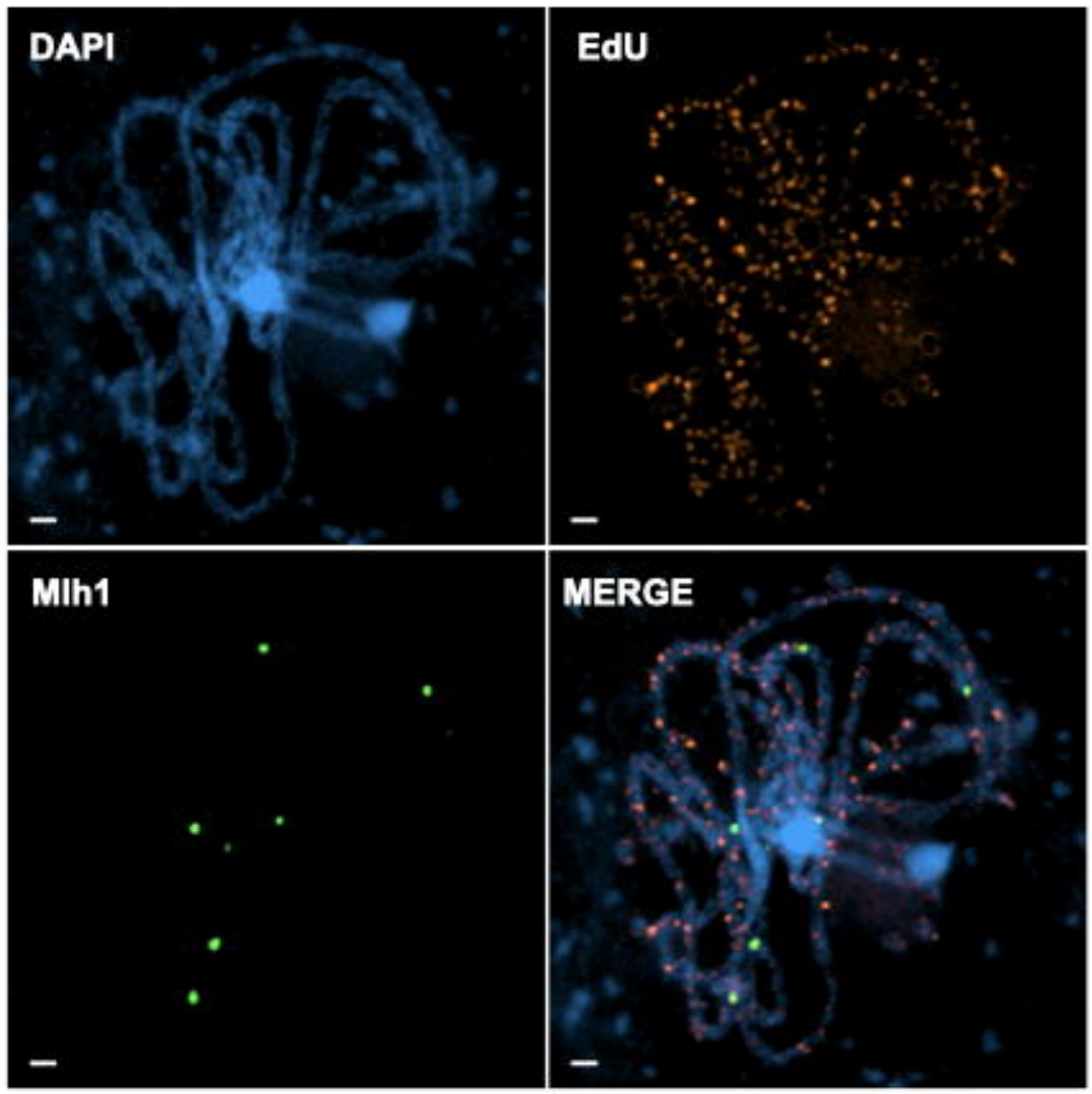

b)

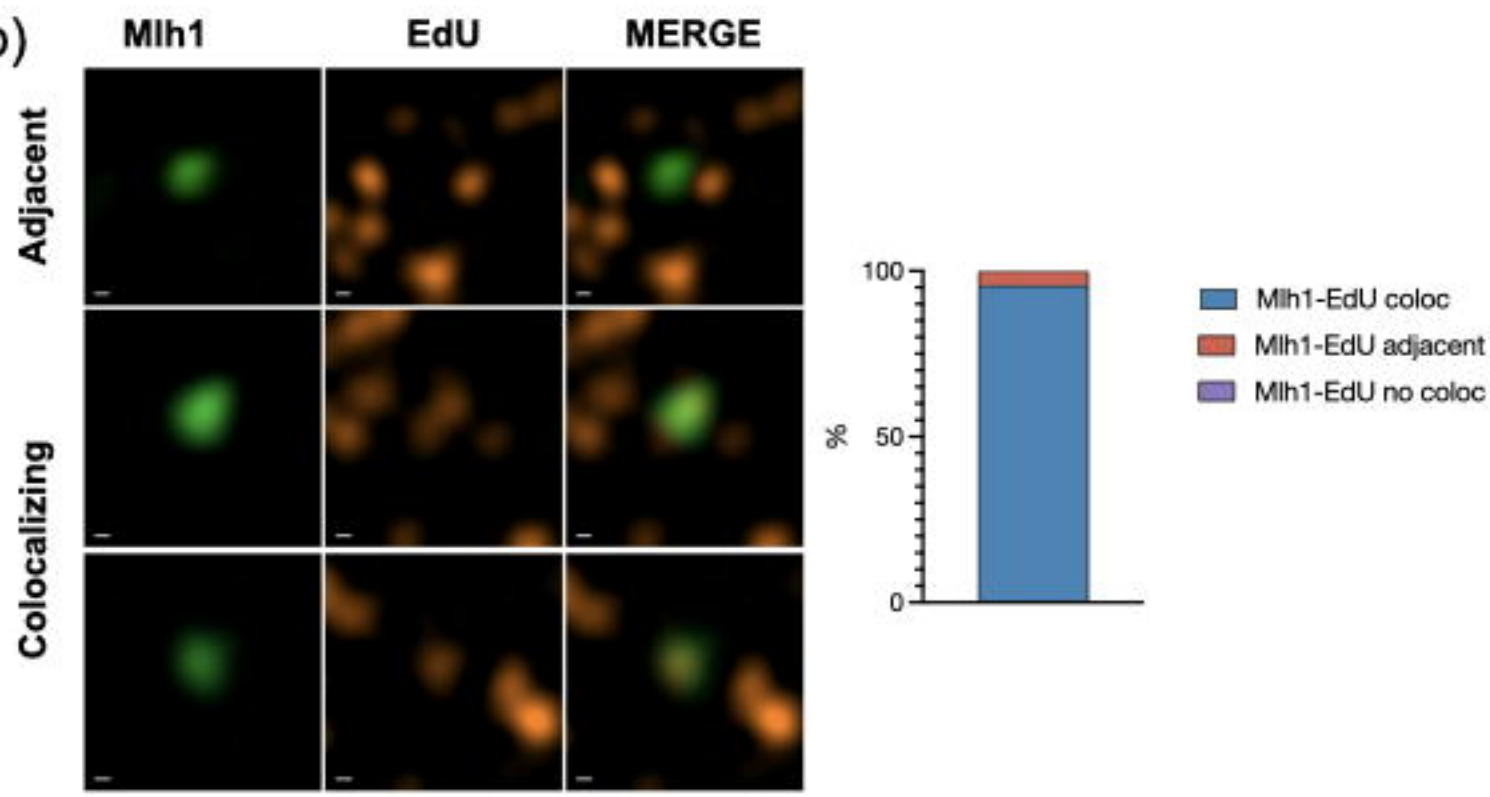

Figure 6. Class I crossovers (CO) colocalize with prophase I DNA synthesis tracts.
a) Wild-type pachytene cell showing DAPI staining (blue), prophase I DNA synthesis tracts (EdU, orange) and Class 1 CO (MLH1, green). b) Examples of colocalising and adjacent MLH1 and EdU foci. The quantification (right) shows that 95.6% of MLH1 foci co-localize with EdU tracts, and the remainder are adjacent to one. a) is a confocal image and b) a single slice of a 3D-SIM image stack. Scale bars are 1μm in (a) and 0.1μm in (b).

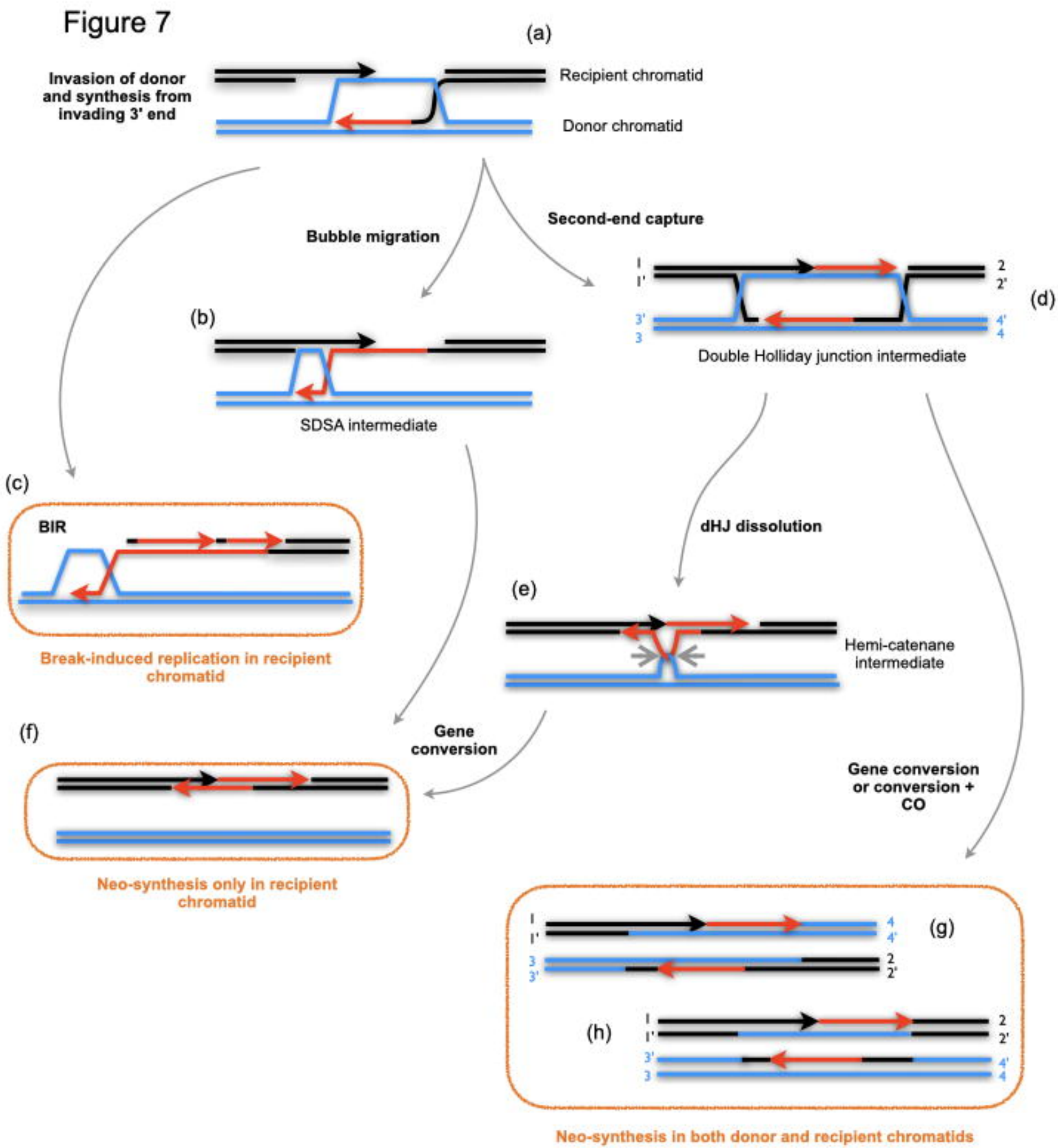

Figure 7. Recombination mechanisms and DNA synthesis tracts.
Following resection and invasion of the donor chromatid (a), DNA neo-synthesis tracts resulting from repair of DSB are expected to be found only on the recipient chromatid in gene conversions (f) resulting from SDSA (b) or dHJ dissolution (e) pathways. A special case of this is the BIR pathway (c), which will result in a long synthesis tract, potentially extending all the way to the end of the recipient chromatid. DNA synthesis tracts are expected to be found on both the recipient and donor chromatids in gene conversions, associated (g) or not (h) to a CO, resulting from resolution of the dHJ intermediate (d).

Figure S1

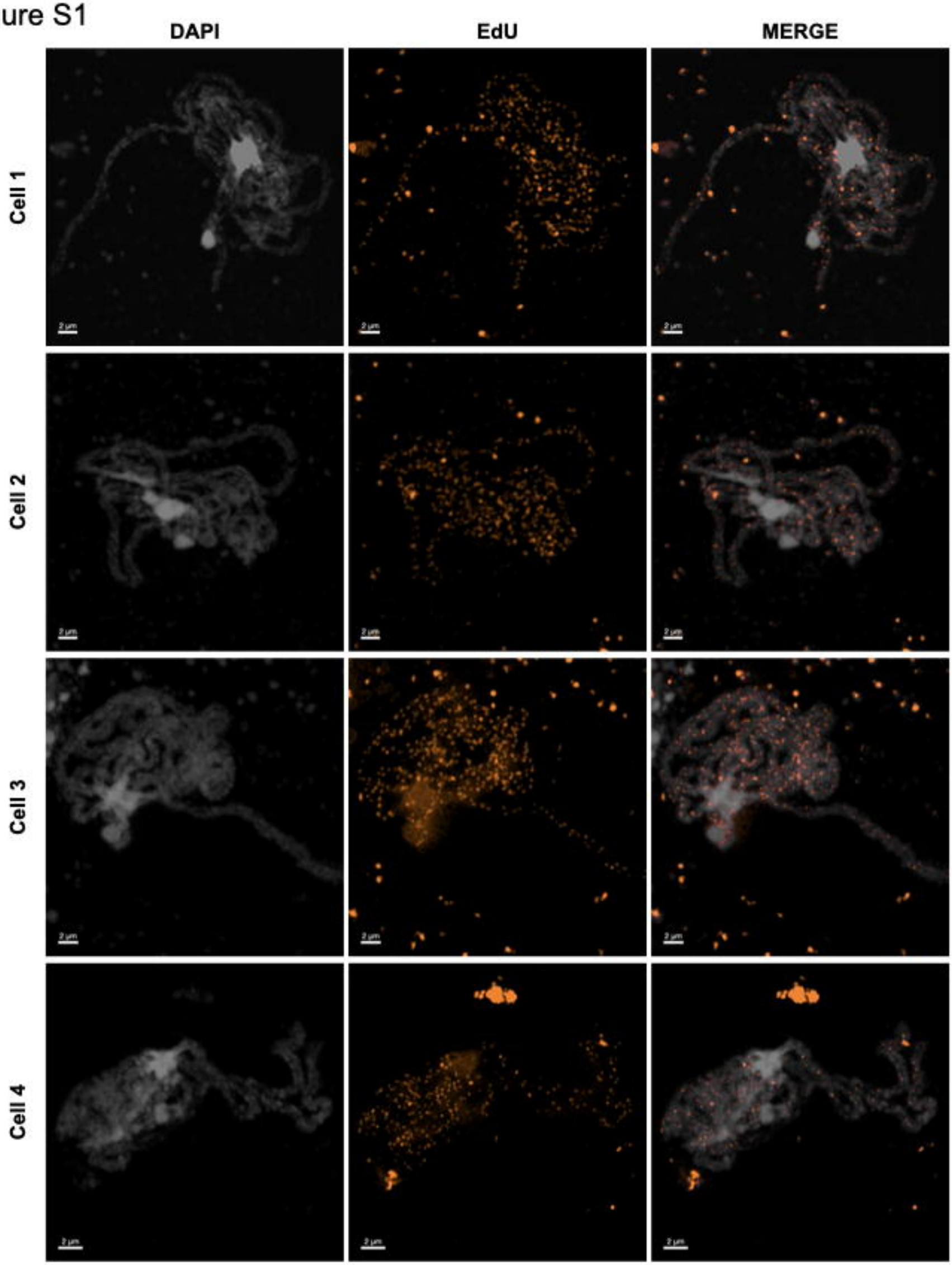

Supplemental Figure S1. Discrete foci of EdU substituted DNA are visible in pachytene chromosomes of Arabidopsis PMC.

Examples of prophase I DNA labelling in pachtene nuclei of wildtype PMC. Each row is the same nucleus, imaged with DAPI fluorescence (white, left), EdU (orange, middle) and the merged image (right). Images taken with the confocal microscope with Airyscan module. 2μm scale bars are included at the bottom left of each image.

Figure S2

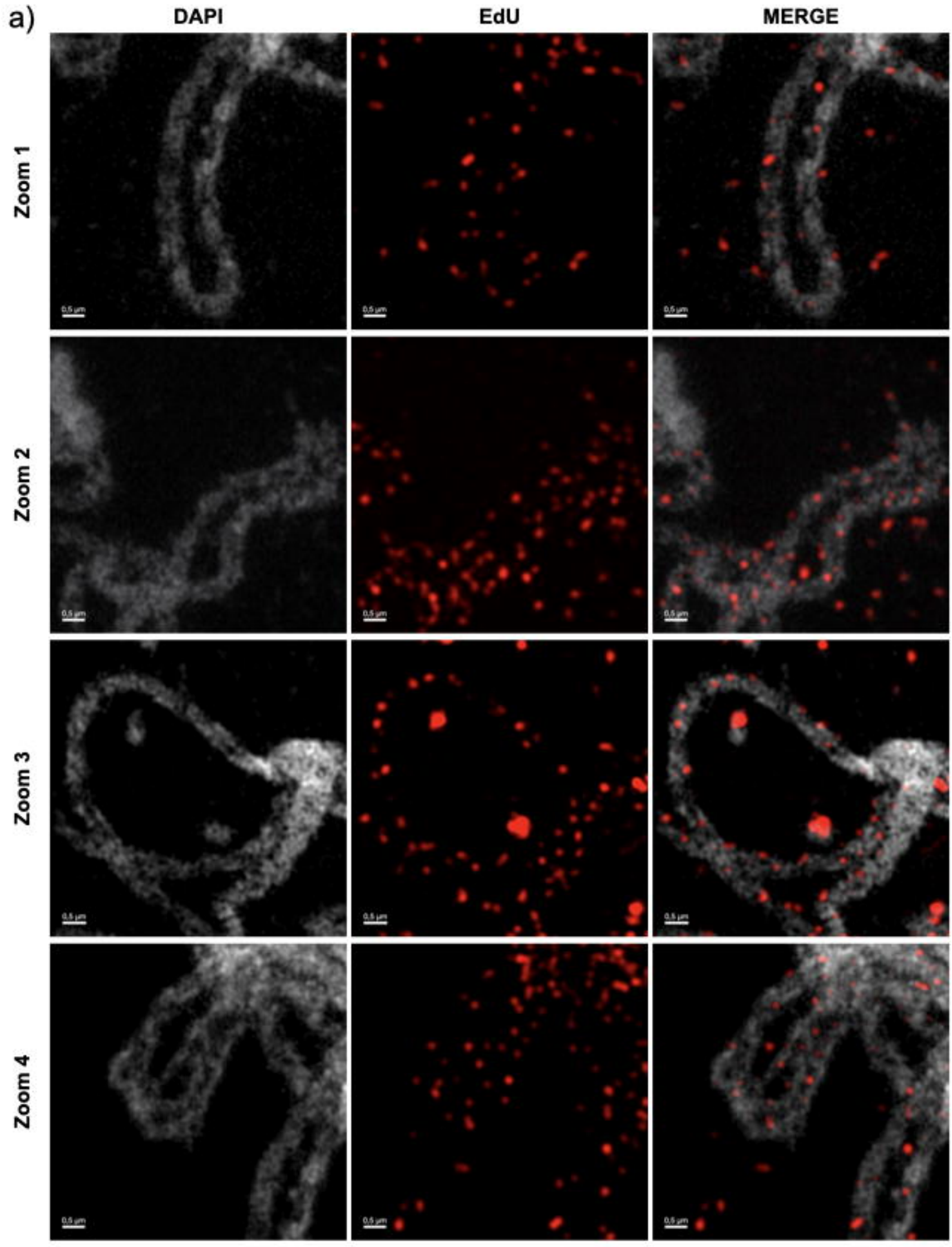

Figure S2

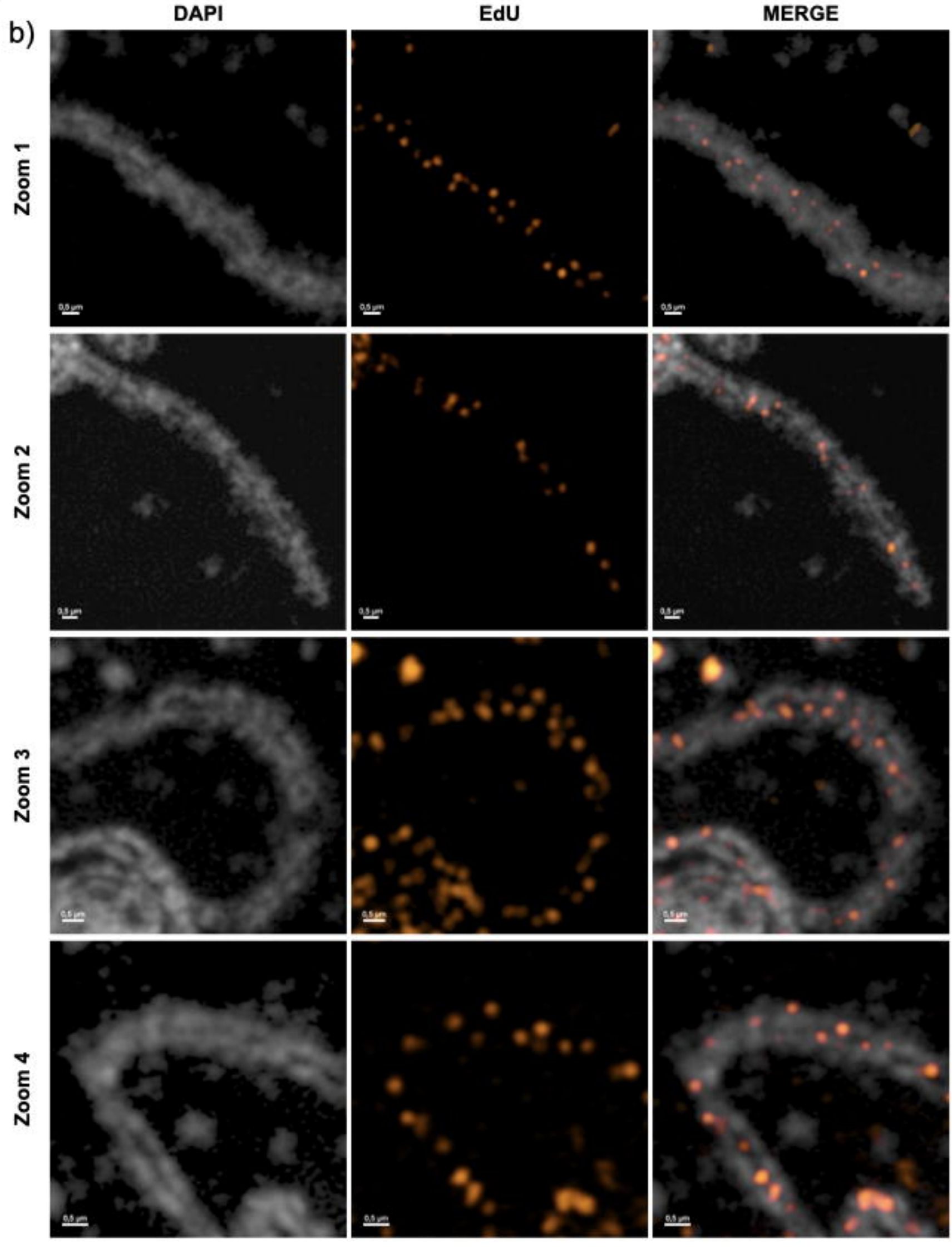

Supplemental Figure S2. Distribution of SPO11-dependent, meiotic DNA synthesis foci on paired pachytene chromosomes from two different cells.
Zoomed regions from SIM (a) and Confocal (b) images of meiotic pachytenes, showing the distribution of EdU-labelled meiotic prophase I DNA synthesis foci (a)red, b) orange) on the DAPI-stained chromosome fibres (white) of the synaptonemal complexes. 0.5μm scale bars are included at the bottom left of each image.